FINAL
CONTRACT REPORT
VTRC 07-CR2

THE IMPACT OF THE AASHTO LRFD DESIGN CODE ON BRIDGE STIFFNESS AND STRENGTH: PART I: METHODS AND DESIGN COMPARISONS

THOMAS T. BABER
Associate Professor

DAVID C. SIMONS
Graduate Research Assistant

Department of Civil and Environmental Engineering
University of Virginia

VTRC
Virginia Transportation Research Council

Http://www.virginiadot.org/vtrc/main/online_reports/pdf/07-cr2.pdf

Standard Title Page - Report on Federally Funded Project

1. Report No.: FHWA/VTRC 07-CR2	2. Government Accession No.:	3. Recipient's Catalog No.:
4. Title and Subtitle: The Impact of the AASHTO LRFD Design Code on Bridge Stiffness and Strength: Part I: Methods and Design Comparisons		5. Report Date: March 2007 6. Performing Organization Code:
7. Author(s): Thomas T. Baber and David C. Simons		8. Performing Organization Report No.: VTRC 07-CR2
9. Performing Organization and Address: Virginia Transportation Research Council 530 Edgemont Road Charlottesville, VA 22903		10. Work Unit No. (TRAIS) 11. Contract or Grant No. 69551
12. Sponsoring Agencies' Name and Address Virginia Department of Transportation 1401 E. Broad Street Richmond, VA 23219 FHWA P.O. Box 10249 Richmond, VA 23240		13. Type of Report and Period Covered Final Contract 14. Sponsoring Agency Code
15. Supplementary Notes		

16. Abstract

The Commonwealth of Virginia is currently transitioning from the long-used AASHTO Allowable Stress Design (ASD) specification to AASHTO's Load and Resistance Factor Design (LRFD) specification. The new specification features revised live loads, more conservative impact factors, a new load distribution method for analysis, and a probabilistically based limit state design approach. Traditional deflection limits have been made optional in the LRFD format. The extensive changes in the specification make it unclear as to whether bridges designed using the LRFD specification will be more or less flexible than those designed using the ASD specification.

A series of bridges were designed using both ASD and LRFD formats to investigate what, if any, significant changes in bridge flexibility might be encountered and whether deflection limits are more or less likely to be violated with the LRFD format. Based upon the design of six single-span bridges with varying spans and numbers of girders, and a partial design of a three-span continuous bridge, it was concluded that the LRFD designs tend to be lighter and more economical in general and also tend to be more flexible than ASD designs of the same bridge. The weight savings appears to be more pronounced on single-span bridges than on multiple-span bridges because of the greater significance of local and lateral stability concerns in the finished bridges for multi-span bridges.

17 Key Words	18. Distribution Statement
Load and Resistance Factor Design, bridge design, bridge design specification	No restrictions. This document is available to the public through NTIS, Springfield, VA 22161.

19. Security Classif. (of this report)	20. Security Classif. (of this page)	21. No. of Pages	22. Price
Unclassified	Unclassified	76	

Form DOT F 1700.7 (8-72) Reproduction of completed page authorized

FINAL CONTRACT REPORT

THE IMPACT OF THE AASHTO LRFD DESIGN CODE ON BRIDGE STIFFNESS AND STRENGTH: PART I: METHODS AND DESIGN COMPARISONS

Thomas T. Baber
Associate Professor

David C. Simons
Graduate Research Assistant

Department of Civil and Environmental Engineering
University of Virginia

Project Manager
Jose P. Gomez, Ph.D., P.E., Virginia Transportation Research Council

Contract Research Sponsored by the
Virginia Transportation Research Council

Virginia Transportation Research Council
(A partnership of the Virginia Department of Transportation
and the University of Virginia since 1948)

In Cooperation with the U.S. Department of Transportation
Federal Highway Administration

Charlottesville, Virginia

March 2007
VTRC 07-CR2

NOTICE

The project that is the subject of this report was done under contract for the Virginia Department of Transportation, Virginia Transportation Research Council. The contents of this report reflect the views of the authors, who are responsible for the facts and the accuracy of the data presented herein. The contents do not necessarily reflect the official views or policies of the Virginia Department of Transportation, the Commonwealth Transportation Board, or the Federal Highway Administration. This report does not constitute a standard, specification, or regulation.

Each contract report is peer reviewed and accepted for publication by Research Council staff with expertise in related technical areas. Final editing and proofreading of the report are performed by the contractor.

ABSTRACT

The Commonwealth of Virginia is currently transitioning from the long-used AASHTO Allowable Stress Design (ASD) specification to AASHTO's Load and Resistance Factor Design (LRFD) specification. The new specification features revised live loads, more conservative impact factors, a new load distribution method for analysis, and a probabilistically based limit state design approach. Traditional deflection limits have been made optional in the LRFD format. The extensive changes in the specification make it unclear as to whether bridges designed using the LRFD specification will be more or less flexible than those designed using the ASD specification.

A series of bridges were designed using both ASD and LRFD formats to investigate what, if any, significant changes in bridge flexibility might be encountered and whether deflection limits are more or less likely to be violated with the LRFD format. Based upon the design of six single-span bridges with varying spans and numbers of girders, and a partial design of a three-span continuous bridge, it was concluded that the LRFD designs tend to be lighter and more economical in general and also tend to be more flexible than ASD designs of the same bridge. The weight savings appears to be more pronounced on single-span bridges than on multiple-span bridges because of the greater significance of local and lateral stability concerns in the finished bridges for multi-span bridges.

FINAL CONTRACT REPORT

THE IMPACT OF THE AASHTO LRFD DESIGN CODE ON BRIDGE STIFFNESS AND STRENGTH: PART I: METHODS AND DESIGN COMPARISONS

Thomas T. Baber
Associate Professor

David C. Simons
Graduate Research Assistant

Department of Civil and Environmental Engineering
University of Virginia

INTRODUCTION

Since approximately 1931, the bridge design standards prescribed by the American Association of State Highway and Transportation Officials (AASHTO) have followed a design philosophy called allowable stress design (ASD), also known as working stress design. Although the detailed specifications have been periodically revised, the philosophy underlying the ASD code has remained the same. Developed with metallic structures in mind, the design methods are based upon elastic behavior. Allowable stresses are calculated by dividing the material yield or ultimate strength by a safety factor. The safety factors are subjectively defined, conservative values that attempt to account for the uncertainty in the design of highway bridges.

In the 1950s, as extensive laboratory data on failure mechanisms of structures began to accumulate, researchers recognized some weaknesses inherent in the concepts of the ASD code. Allowable stress codes do not permit design directly against the actual failure limit states, unless those limit states occur within the elastic range. This limitation applies for all materials where inelastic behavior occurs at the onset of failure. Even nominally isotropic homogeneous materials such as steel do not behave in a linearly elastic manner in the failure region, either as a consequence of material nonlinearity, or instability, or some combination of the two. Thus a limit state design approach is preferable. The first generation of AASHTO code to use a limit state method for design of steel structures, called load factor design (LFD), was introduced in the 1970s as an alternative to the ASD specifications. The LFD specification retained the ASD load model and did not consider differing levels of uncertainty in structural resistance models, but for the first time permitted design directly against the failure state, instead of against fictitious allowable stress states.

In addition to its failure to adequately address failure limit states, the ASD design approach does not provide a consistent measure of strength through the use of probabilistically derived safety factors, which is a more suitable measure of resistance than is a fictitious allowable stress. In particular, since the safety factors are only applied to resistance, the

differing levels of variability in the various load components cannot be adequately taken into account within the ASD format.

In light of these shortcomings, researchers began developing new design specifications that use the probabilistic concepts that have been the subject of intensive research beginning around 1969 (Melchers, 2001). In 1986, AASHTO began studying ways to incorporate load and resistance factor design (LRFD) philosophies into the standard specifications. This effort resulted in the first edition of the AASHTO *LRFD Bridge Design Specifications* (AASHTO, 1994). This LRFD bridge design code was adopted with a provision to consider phasing out the ASD specifications in the near future. The second edition was introduced in 1998, and the third edition became available in July, 2005. As discussed by Kulicki (2005), the development process has been lengthy and is still underway.

In addition to new reliability based design philosophies, and the introduction of a more sophisticated limit state approach to categorizing structural resistance, the AASHTO 2nd Edition LRFD bridge design code (AASHTO, 1998) contained numerous changes in loads and load applications, when compared to the AASHTO 15th Edition ASD code (AASHTO, 1992) and the 17th Edition (AASHTO, 2002). These changes include a revamped live load model, a newly derived set of load distribution factors, and a new, and slightly more conservative, set of impact factors (now called dynamic load allowances. These changes are briefly discussed here.

Dating back to the 1940s, AASHTO had used three basic live load models to approximate the vehicular live loads that would be experienced by a bridge: the H or HS design trucks, the design tandem, and the design lane loading. The HS design truck, or standard truck, is a three-axle truck intended to model a highway semitrailer. The design tandem is a two-axle loading intended to simulate heavy military vehicles. The design lane loading primarily consists of a distributed load meant to control the design of longer spans where a string of lighter vehicles, together with one heavier vehicle, might produce critical loads. In the AASHTO ASD codes (AASHTO, 1992, 2002), each of these load models was applied individually. Before the implementation of the new LRFD code, Kulicki and Mertz (1992) and Nowak (1993) conducted weigh-in-motion studies to survey the effects of vehicular live loads on over 10,000 existing structures. Nowak and Hong (1991) conducted extensive simulation studies of static moments, and reported a statistical analysis of those moments caused by 10,000 surveyed trucks on bridges of differing spans that had been reported by previous researchers (Agarwal and Wolkowicz, 1976). Subsequently, AASHTO used the results of the truck data, together with a statistical extrapolation to a 75-year design life, to provide the basis for the AASHTO LRFD design loading. These extensive modifications of the vehicular load models are discussed comprehensively by Nowak (1999). Significantly, Nowak and Hong (1991) reported 75-year mean maximum design moments significantly greater than the HS20-44 bending moments on the same structures based upon their simulations. The results of these studies indicated that the AASHTO ASD live load models consistently underestimated the load effect of vehicles on the road today. However, Nowak (1993) found that applying the design truck *in combination with* the design lane loading produced load effect magnitudes comparable to those of the measured vehicles. Thus, the AASHTO LRFD contains two live load models with the design lane superimposed upon them, the design truck and the design tandem. This is expected to produce significantly increased design loads.

The second notable change in vehicular load modeling between the ASD and LRFD codes is the method used to approximate the live load amplification due to dynamic loading. The dynamic load allowance, formerly referred to as the impact factor, is an equivalent static magnification factor to be applied to a statically applied load on a structure in order to predict the additional response amplitude resulting from the motion of the load across the structure. In a highway bridge, the actual dynamic response amplitude is a function of a number of factors. Such factors include, but are not limited to bridge span, type (continuous or simple span), number of girders, slab stiffness, bridge damping, deck roughness, vehicle mass, vehicle velocity, damping, number of axles, suspension system, vertical velocity upon entering the bridge, probability of coincidence of maximum load and maximum impact, and position of load relative to a girder (Hwang and Nowak, 1991). In an attempt to simplify this dynamic behavior, the AASHTO ASD specifications provided an impact factor that varies with the length of the bridge, but is to be no greater than 0.3. The new LRFD specifications simplify the model even further by providing constant dynamic load allowances: 0.33 for strength limit states of all members, 0.75 for deck joints, and 0.15 for fatigue (Taly, 1998).

The manner in which loads are transmitted to each girder is a third modeling consideration that was revised with the adoption of the LRFD code. The response of a bridge to a passing vehicle is a complex deformation, in which a portion of the load is transferred to each of the supporting girders. The exact proportion of the load carried by each girder is a function of the girder spacing, span length, slab stiffness, the number and locations of cross frames, and the placement of the load on the span. Both the AASHTO ASD and LRFD codes permit the use of distribution factor methods to model the transfer of loads through the slab to each girder. The AASHTO ASD distribution factors were originally developed using orthotropic plate theory, and the resulting equations are based upon the girder spacing alone. These ASD distribution factors are plagued by inconsistency, sometimes being overly conservative and at other times being non-conservative. In an attempt to more accurately model the distribution of loads, Zokaie et al. (1991, 2000) developed the LRFD distribution factors, which consider span length and girder stiffness as well as girder spacing. It is difficult to predict how the use of LRFD distribution factors will affect the final design moments and shears, in view of the relatively inconsistent results produced by the ASD distribution factors.

If the remainder of the design specification remained unchanged, the significantly increased vehicular live loads would likely lead to stronger and stiffer structures. However, these changes in the load approximations are accompanied by new, strength-based design procedures. Such strength-based procedures have often led to more flexible structures in the past, so it is uncertain whether the increased loads will result in a comparable increase in bridge strength and stiffness. The revised load distribution factors further complicate the situation.

A key issue in the application of the new specification is the flexibility of the resulting designs. For a number of years, it has been observed that some steel-concrete composite bridges that have been designed according to AASHTO ASD standards have a tendency to display excessive flexibility. While the term “excessive flexibility” is somewhat subjective, and is often based upon the perceptions passengers in autos on the bridges, there may be more serious consequences for the bridge. Some bridges that have been observed to be too flexible also appear to have exhibited relatively rapid deterioration of wearing surfaces, and higher than

expected maintenance costs. Whether there is any direct relation between the perceived flexibility of the bridge and the apparently higher rates of deck deterioration is not certain, but is consistent with observations that have been made over a number of years, by numerous engineers. A summary paper (ASCE, 1958) indicated that, based upon available data at that time, bridge deflections were not considered to be a serious problem, except insofar as potential passenger/pedestrian discomfort were concerned. Wright and Walker (1971) also summarized deflection limits on bridges. In recent years, most of the work related to deflection control has focused upon the passenger/pedestrian discomfort question. Little work on any relationship between durability and bridge flexibility appears to have been done since that time, although one of the recommendations of ASCE (1958) was specifically directed toward addressing this question. However, in the intervening years, there have been significant changes in the design of bridges. First, there has been an increasing trend to use higher strength steels in all bridges, which inherently leads to more flexible structures. Second, the development of LFD and more recently LRFD design have lead to somewhat lighter-weight and potentially more flexible structures.

The source of excessive deflections in bridges could, trivially, be traced to the somewhat arbitrary choice of deflection limitations that has been imposed by AASHTO specifications (L/800 in the case of girder bridges under traffic loads). However, the situation may be more complex. Specifically, the loadings upon which highway bridge design has been based for a number of years have been in existence since at least 1944. In the intervening years, there has been a significant observed increase in average daily truck traffic (ADTT) on many roads, and a significant increase in the observed weights of many trucks. While load limits are in place to ostensibly prevent bridge stresses from exceeding design stresses, it is well known that many overweight trucks avoid weigh stations. Therefore, it is likely that many bridges on heavily traveled routes are subjected to more cycles of high stress, and quite possibly to higher stresses than the ASD HS-20 loading is intended to represent. The correct value of dynamic load allowances, formerly known as impact factors, has also been called into question by numerous researchers in recent years. The revised loadings and dynamic load allowances in the LRFD specification may address these issues, but it is not clear that this is the case.

In addition to the presence of increased vehicular loadings, trends in bridge design over the last 50 years have tended toward more flexible bridge structures, so the L/800 limit, which has also been existence for many years, may in fact need to be modified. The original L/800 limit appears to have been based upon non-composite bridges, and the calculated deflections for such bridges were based upon the girder stiffness only, even though the actual bridges displayed considerable composite action in the field. More recent design practice has explicitly included composite behavior in the design stage, and the stiffness estimates have been based upon the composite section. Therefore, application of the L/800 deflection limit to composite bridges may tend to permit significantly greater flexibility than would have been allowed in previous "non-composite" bridges that actually displayed significant composite action (ASCE, 1958). Additional trends tending to contribute to greater flexibility include use of higher strength steels, which permit the use of smaller sections. Therefore, it is important to determine just how important the optional deflection provisions are, and whether more stringent guidelines should be followed in some circumstances.

PURPOSE AND SCOPE

Given the numerous differences between the AASHTO ASD and LRFD highway bridge design codes, and the steel-concrete composite sections in particular, it is important that the Commonwealth of Virginia determine the manner in which these code changes affect the design of composite steel girder-slab bridges. This is particularly important in view of the observed flexibility of many composite steel girder-slab bridges, and the apparent tendency of some composite steel girder-slab bridges toward premature deck deterioration. It is the purpose of this study to evaluate the significance of those changes. Toward this end, the following questions are addressed in the current report:

1. Does the increase in vehicular live load proposed by the AASHTO LRFD specification lead to stronger and stiffer composite bridges, and decrease the likelihood that deflections will control the design?

2. How do the new distribution factors, taken together with the new AASHTO LRFD loadings influence the eventual girder design moments and shears?

3. Is the reduction of the deflection limits to optional status justified, or should the limits be made mandatory for composite bridges designed within the Commonwealth of Virginia, and possibly made more stringent?

4. How do the new strength-based design methods affect the dynamic characteristics of composite bridges, and what sort of failure modes can be expected.

METHODS

Overview

To address these questions, a series of design studies were conducted using the 2nd Edition AASHTO LRFD Specification and, for comparison purposes, the 17th Edition AASHTO ASD Specification. Within the scope of the study, all bridges considered were multilane, composite steel girder-slab bridges, similar to those that might be encountered on an interstate highway system.

Several bridges of different spans covering the range most commonly encountered in practice were selected for "design." Considering the large number of parameters that can be varied, the study was limited to include 4, 5, and 6 girder bridges. In order to simplify the comparison between the two AASHTO design codes, the same deck plan design was used in each case, with the thickness only varying with the number of girders, as outlined in Appendix D. Simply supported bridges with spans of 22.87 m (75 feet) and 45.73 m (150 feet) were designed. A three span continuous bridge with 30 m, 50 m and 30 m spans was also considered. To allow the design effort to focus upon the steel girders, all bridges were taken as 14.18 m (46.5 feet) wide, with a 13.42 m (44 feet) wide roadway. and 990 mm (3.25 ft) distance from center of

exterior girders to edge of bridge. Selecting these dimensions not only provided representative spans for design, but also allowed direct comparison with designs presented elsewhere (Barker and Puckett, 1997). Skew bridges were not considered within the current study. Design of cross frames, transverse stiffeners, and bearing stiffeners are included. However, the use of longitudinal web stiffeners is not investigated. Hybrid girders were also not considered. More comprehensive cost optimization studies could consider longitudinal stiffeners, but are beyond the scope of the present study.

Partial designs of the bridges were performed using the 2d Edition AASHTO LRFD specification as a basis. To provide a basis for comparison, the bridges were then re-designed using the 17th Edition AASHTO ASD specification. It was important that bridges being compared be designed to a similar level of optimality, relative to the relevant specifications. Therefore, it was most suitable for the studies to select hypothetical bridges of similar bridge cross-section but with different span lengths. The designs were not fully detailed to permit construction, since a number of aspects of bridge design, such as shear stud spacing and substructure design do not significantly influence the response parameters of interest in the current study. However sufficient information was obtained about the deck and girder dimensions and diaphragm locations and dimensions to permit reasonable finite element models to be constructed for the bridge superstructures. Typically, the bridges chosen for comparative design were of a scope consistent with interstate highway application.

Once each composite bridge design was completed, numerous comparisons were made between the ASD and LRFD designs. Since the LRFD code changes include modified vehicular loads, modified distribution factors, and modified dynamic load allowances (impact factors), and it was desirable to trace any systematic changes that occurred through the design process, quantities calculated during the development of the design were also considered. The following comparisons were conducted:

1. the vehicular live loads used in design
2. the dynamic load allowances used in design
3. the distribution factors used in design
4. the amount of steel required for each bridge
5. the maximum live load deflection of each bridge under service loads.

The vehicular live loads, dynamic load allowances, distribution factors, and the amount of steel required for each bridge were quantities inherently embedded in each of the bridge designs, and were selected as appropriate points of comparison between the two designs. In addition, fundamental dynamic properties of each designed bridge were calculated, including

1. the lowest bending natural frequencies of each bridge
2. the additional mode shapes obtained through a modal analysis.

These dynamic response characteristics are reported elsewhere (Simons, 2005; Baber and Simons, 2005).

Design Methods

General Considerations

The design calculations were lengthy, and are not covered in full detail in this report. However certain aspects of the design process provide insight into some of the major changes introduced by the LRFD code, and are worthy of discussion, while other aspects of the design process provide some useful practical guidelines for engineers. Wollman (2004a,b) provides a two-part discussion of the LRFD design approach that provides valuable background.

It was important that LRFD and ASD designs be completed to a relatively similar level of economy, and optimality in the study, since otherwise any detailed comparison of the designs would be meaningless. During the project, computer software that would have greatly simplified the procedure was not available, so the designs were completed using hand calculations. Although this reduced the number of designs that could be compared, it did allow the researchers to develop a good deal more insight into the design process. In the remainder of the discussion, attention is focused upon the LRFD design, since most readers are familiar with the ASD design of composite steel girder/concrete slab bridges. Additional detail on the ASD designs may be found in Simons (2005).

AASHTO (1998) indicates that all girders must be designed against the following limit states:

1. the strength limit state flexural resistance (LRFD section 6.10.4)
2. the serviceability limit state control of permanent deflection (LRFD section 6.10.5)
3. the fatigue and fracture limit state for details (LRFD section 6.6.3)
4. the fatigue limits for webs (LRFD section 6.10.6)
5. the strength limit state for shear (LRFD section 6.10.7)
6. the constructability strength requirement (LRFD section 6.10.3.2)
7. optionally, the deflection provisions (LRFD section 2.5.2.6.2),

Of these provisions, the two that tended to control the size of the beam section in the present studies were found to be limit states 1 and 2 (flexural strength and permanent deflection control). The shear strength limit state (limit state 5) determined the transverse stiffener requirements, but did not require an increase in web thickness in the present studies. The constructability strength requirement could be met in all designs considered here by appropriate spacing of intermediate cross-frames, or temporary construction bracing. In other cases, lateral stability requirements might require modification of the girder cross-section. The fatigue limit state for webs may occasionally require that the web thickness be increased, but did not seem to control the overall design in the present studies. Therefore, the overall design procedure that was followed in the present studies was to begin with the flexural strength requirements (limit state 1), then check the serviceability limit state (limit state 2), followed by web fatigue limits (limit state 4). Subsequently, the constructability provision was checked to determine bracing requirements, and the transverse stiffener spacing was determined by checking the shear limit state provisions (limit state 5). The bridges were not fully detailed, so only limited detail fatigue checks were conducted. The deflection limits were not imposed during the design, since they are

considered optional, but the deflections were subsequently calculated, to determine if those limits would be violated.

Preliminary Design

Because the designs in the current study were completed using hand calculations, it was essential that the first estimates of girder section dimensions be made as efficiently as possible. It was undesirable to begin design iterations with sections that were either far too large, or far too small. Therefore, a considerable amount of time was spent at the beginning of the project evaluating different ways of estimating girder cross-section dimensions. Generally, it was found that efficient girders could be obtained if the girder web height D was kept near the minimum recommended by AASHTO. Hence, designs tended to have span to depth ratios on the order of 24 to 30. This also tended to provide a critical test for the deflection criteria of the LRFD codes, since shallower girders will tend to lead to more flexible structures. The preliminary sizing tools discussed below allow estimation of girder cross-section requirements regardless of the ratio, however. The specific ratios used in the estimation procedures given below are provided only as guidelines for a general approach to section sizing. As additional insight and design experience is gained, engineers should feel free to adjust the ratios to suit their personal experience.

Positive bending plastic moment capacity estimation of girder cross-sectional area:

For a composite girder in positive bending, the depth of web in compression, D_c, is typically small in the composite state. Therefore web buckling is not a problem in the composite state. The compression flange is supported both laterally and locally, so neither local flange buckling nor lateral torsional buckling is an issue. Therefore, assuming that the engineer chooses to design the section using the plastic capacity and that the plastic moment can be reached in the composite state, a reasonable first estimate of the steel girder area is obtained using a simplified plastic moment calculation. This approach allowed subsequent detailed calculations to converge rapidly to the final design section. The following assumptions were found to provide a reasonable first estimate in many cases:

1. All of the compression is in the slab.
2. The girder is totally in the tension zone.
3. The compression flange area is approximately $0.5A_B$, where A_B is the tension flange area.
4. The web area is approximately $2A_B$, in order to achieve the minimum web thickness ratios.
5. The flange thicknesses are between .01D and .02D, where D is the web height.

Assumptions 1 and 2 should be valid for composite girders, provided the spans are not too long. The exact point at which the assumption becomes invalid occurs when the tension capacity of the minimum steel section exceeds the compressive capacity of the available concrete slab area. If the steel tension capacity is not too much larger than the concrete compression capacity, the error of using this assumption for first estimates will not be very large, since the compression flange will be located very near the plastic neutral axis (PNA), so it will not

contribute much to the plastic moment either way. If the PNA starts to move significantly into the web, a different set of assumptions may be needed.

Assumption 3, is based upon two observations. For composite design, it is possible for the compression flange to be significantly smaller than the tension flange, since its primary function in the final state is to transfer the load from the steel to the concrete slab. However it cannot be made too small, because of lateral torsional buckling considerations in the non-composite stage, and because of the code imposed limits on relative lateral bending stiffness of the tension and compression flanges. The value 0.5 appears to be near the minimum value that permits these two limits to be met. Since the objective of the estimate is to bound the section size from below, it is desirable to pick as small a tension flange as may ultimately be feasible. There is, however, nothing magic about the 0.5 value, and engineers may wish to use slightly larger values, based upon personal experience.

Assumption 4 was established after several preliminary designs were conducted using different trial ratios. Generally for plate girders without longitudinal stiffeners, which are the focus of the current study, web depth-thickness ratios prevent the web from being much smaller than this. Likewise, assumption 5 was developed after some trial and error. Perhaps the greatest value of the approach is not in the specific ratios chosen (although these values did work well in the studies reported on herein) but in a general approach to preliminary section bounding based upon some simple hand calculations.

Given the assumptions, a limiting capacity of the beam may be calculated. At the plastic moment, it is reasonable to estimate that the moment arm of the *C*-*T* couple is approximately

$$l_c \approx 0.6D + t_h + 0.5t_s \qquad [1]$$

In this equation, the thickness of the haunch, t_h, and the thickness of the structural portion of the slab, t_s, are assumed to be previously known from the slab design. If only a portion of the slab is in compression, l_c will increase slightly (by no more than $t_s/2$). If only a portion of the steel is in tension, l_c will decrease slightly.

Since the girder is assumed to be completely in tension, the effective tension force is given by

$$T \approx F_y(A_B + 2A_B + 0.5A_B) = 3.5A_BF_y \qquad [2]$$

and the section plastic moment capacity of the section is approximately

$$M_p = l_cT = \left(0.6D + t_h + 0.5t_s\right)\cdot 3.5A_BF_y \qquad [3]$$

Although the strength I criterion may not be the controlling criterion, it certainly is *necessary* that it be satisfied. Therefore, a reasonable estimate of a lower bound on the section area is obtained from the strength I criterion.

$$\phi_b M_p \geq \eta\left[1.25M_{D_1} + 1.5M_{D_2} + 1.25M_{D_3} + 1.75\left(M_{La} + (1+I)M_{Tr}\right)\right] \qquad [4]$$

For flexure, the resistance factor is specified by AASHTO as ϕ=1. For the designs in the current study, the load modifier was taken as $\eta = 0.95$. Substituting the approximate expression for M_p then yields the result

$$A_B \geq \frac{\eta\left[1.25M_{D_1} + 1.5M_{D_2} + 1.25M_{D_3} + 1.75\left(M_{La} + (1+I)M_{Tr}\right)\right]}{3.5F_y(0.6D + t_h + t_s/2)} \qquad [5]$$

or, if it is preferred to work directly in terms of the total girder area,

$$A \geq \frac{\eta\left[1.25M_{D_1} + 1.5M_{D_2} + 1.25M_{D_3} + 1.75\left(M_{La} + (1+I)M_{Tr}\right)\right]}{F_y(0.6D + t_h + t_s/2)} \qquad [6]$$

The area obtained from this calculation will be near the smallest possible value achievable for a given *D*. Some variation from this value may occur, depending upon the actual ratio of the web area to bottom flange area, and the actual location of the plastic neutral axis. Apparently, from the above calculation, *A* will decrease as *D* increases. Such behavior is obviously what should happen, and the fact that equations [5] and [6] show this trend suggests that they are not unreasonable. However, minimum web D/t_w ratios, and construction considerations will limit the amount of efficiency that can be gained by increasing *D*. It was typically found that, in the absence of longitudinal stiffeners, the shallowest girders (span to depth of girder ratio of roughly 28-30) were either the lightest weight, or nearly so in the designs carried out within the current project. If longitudinal stiffeners are used, the limiting web thickness ratios will change. Then deeper girders may be lighter weight and provide greater stiffness.

Elastic Section Calculations to Estimate Girder Properties, Positive Bending

The plastic section properties may not control the design of a section, or the engineer may decide not to allow use of plastic section resistance, even if the compactness ratios are locally satisfied. The first situation may occur if the serviceability II criterion controls the design, in which case the area may need to be increased relative to that predicted for adequate plastic moment capacity. The latter situation may occur in a multi-span girder if the negative moment regions are not compact, and is discussed more fully below.

In either case, it is desirable to have available procedures for estimating elastic section properties. A reasonable estimation procedure is illustrated below. The basic variables are taken as the tension flange area A_{tf} and the web depth *D*. The effective slab dimensions are assumed known, as is the modular ratio *n*. The ratios of the web area, compression flange area, and slab area to the tension flange area are assumed to be α_w, $\alpha_{cf,}$ and α_{sl} respectively. The ratio of the tension flange thickness and the compression flange thickness to *D* are taken as γ_{tf}, and γ_{cf}

respectively. The distance from the top of the beam to the center of the slab is taken as $\beta_{sl}D$. These quantities are illustrated in Figure 1.

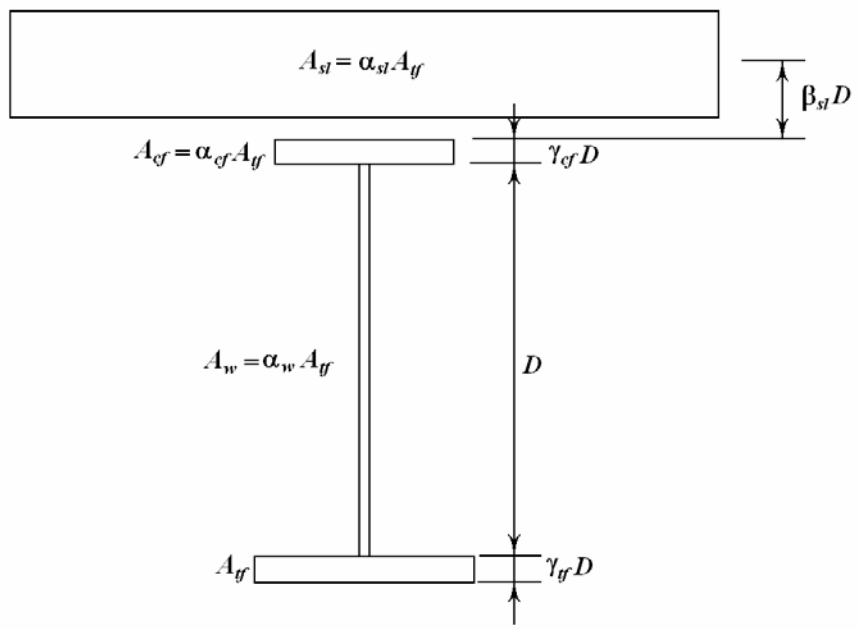

Figure 1. Cross-section properties for estimating minimum section requirements in positive bending

The calculations are relatively insensitive to γ_{tf}, and γ_{cf}, which tend to be between 0.01 and 0.02, and 0.02 was used in the current studies. For a first estimate, β_{sl} may be taken as approximately

$$\beta_{sl} \approx \frac{15t_s + 30t_h}{L} \qquad [7]$$

where L is the span of the girder. A good starting estimate for α_{cf} is around 0.5, and for α_w is typically around 1.5-2.5. A reasonable value of α_{sl} is the most difficult quantity to estimate accurately, but a starting value of about 40 appears to be reasonable, and a second iteration can be used to improve the estimate if the first guess is too far off. Once nominal values of the dimensionless ratios have been chosen, the section properties can be calculated as functions of A_{tf} and D only. For the non-composite section,

$$\begin{aligned} \bar{y}_b &= C_{0_{NC}} D \\ I_{NC} &= C_{1_{NC}} A_{tf} D^2 \\ S_{T_{NC}} &= C_{T_{NC}} A_{tf} D \\ S_{B_{NC}} &= C_{B_{NC}} A_{tf} D \end{aligned} \qquad [8]$$

where $C_{0_{NC}}, C_{1_{NC}}, C_{T_{NC}}, C_{B_{NC}}$ are dimensionless coefficients, defined below, and

$\bar{y}_b$ = distance from the extreme bottom fiber to the neutral axis
I_{NC} = non-composite moment of inertia
$S_{T_{NC}}$ = non-composite top section modulus
$S_{B_{NC}}$ = non-composite bottom section modulus

In equations [8], the coefficients are given by

$$
\begin{aligned}
C_{0_{NC}} &= \frac{0.5\gamma_{tf} + (\gamma_{tf} + 0.5)\alpha_w + (1 + \gamma_{tf} + 0.5\gamma_{cf})\alpha_{cf}}{1 + \alpha_w + \alpha_{cf}} \\
C_{1_{NC}} &= \left[\left(C_{0_{NC}} - 0.5\gamma_{tf}\right)^2 + \frac{\alpha_w}{12} + (C_{0_{NC}} - \gamma_{tf} - 0.5)^2 \alpha_w + (1 + \gamma_{tf} + 0.5\gamma_{cf} - C_{0_{NC}})^2 \alpha_{cf} \right] \\
C_{T_{NC}} &= \frac{C_{1_{NC}}}{(1 + \gamma_{tf} + \gamma_{cf}) - C_{0_{NC}}} \\
C_{B_{NC}} &= \frac{C_{1_{NC}}}{C_{0_{NC}}}
\end{aligned}
\qquad [9]
$$

The long-term composite section properties are

$$
\begin{aligned}
\bar{y}_{b_{LT}} &= C_{0_{LT}} D \\
I_{LT} &= C_{1_{LT}} A_{tf} D^2 \\
S_{T_{LT}} &= C_{T_{LT}} A_{tf} D \\
S_{B_{LT}} &= C_{B_{LT}} A_{tf} D
\end{aligned}
\qquad [10]
$$

In equations [10],

$\bar{y}_{b_{LT}}$ = Distance from bottom of beam to long-term composite neutral axis
I_{LT} = Long-term composite moment of inertia
$S_{T_{LT}}$ = Long-term composite top section modulus
$S_{B_{LT}}$ = Long-term composite bottom section modulus

and

$$
C_{0_{LT}} = \frac{0.5\gamma_{tf} + (\gamma_{tf} + 0.5)\alpha_w + (1 + \gamma_{tf} + 0.5\gamma_{cf})\alpha_{cf} + \left(1 + \gamma_{tf} + \gamma_{cf} + \beta_{sl}\right)\frac{\alpha_{sl}}{3n}}{1 + \alpha_w + \alpha_{cf} + \frac{\alpha_{sl}}{3n}}
$$

$$
\begin{aligned}
C_{1_{LT}} &= \left(C_{0_{LT}} - 0.5\gamma_{tf}\right)^2 + \frac{\alpha_w}{12} + (C_{0_{LT}} - \gamma_{tf} - 0.5)^2\alpha_w \\
&\quad + (1 + \gamma_{tf} + 0.5\gamma_{cf} - C_{0_{LT}})^2\alpha_{cf} + \frac{\alpha_{sl}}{3n}(1 + \gamma_{tf} + \gamma_{cf} + \beta_{sl} - C_{0_{LT}})^2 \\
C_{T_{LT}} &= \frac{C_{1_{LT}}}{(1 + \gamma_{tf} + \gamma_{cf}) - C_{0_{LT}}} \\
C_{B_{LT}} &= \frac{C_{1_{LT}}}{C_{0_{LT}}}
\end{aligned}
\qquad [11]
$$

The short-term composite section properties are estimated as

$$
\begin{aligned}
\bar{y}_{b_{ST}} &= C_{0_{ST}} D \\
I_{ST} &= C_{1_{ST}} A_{tf} D^2 \\
S_{T_{ST}} &= C_{T_{ST}} A_{tf} D \\
S_{B_{ST}} &= C_{B_{ST}} A_{tf} D
\end{aligned}
\qquad [12]
$$

where

$$
C_{0_{ST}} = \frac{0.5\gamma_{tf} + (\gamma_{tf} + 0.5)\alpha_w + (1 + \gamma_{tf} + 0.5\gamma_{cf})\alpha_{cf} + \left(1 + \gamma_{tf} + \gamma_{cf} + \beta_{sl}\right)\frac{\alpha_{sl}}{n}}{1 + \alpha_w + \alpha_{cf} + \frac{\alpha_{sl}}{n}}
$$

$$
\begin{aligned}
C_{1_{ST}} &= \left(C_{0_{ST}} - 0.5\gamma_{tf}\right)^2 + \frac{\alpha_w}{12} + (C_{0_{ST}} - \gamma_{tf} - 0.5)^2\alpha_w \\
&\quad + (1 + \gamma_{tf} + 0.5\gamma_{cf} - C_{0_{ST}})^2\alpha_{cf} + \frac{\alpha_{sl}}{n}(1 + \gamma_{tf} + \gamma_{cf} + \beta_{sl} - C_{0_{ST}})^2 \\
C_{T_{ST}} &= \frac{C_{1_{ST}}}{(1 + \gamma_{tf} + \gamma_{cf}) - C_{0_{ST}}} \\
C_{B_{ST}} &= \frac{C_{1_{ST}}}{C_{0_{ST}}}
\end{aligned}
\qquad [13]
$$

Although the coefficients in these equations appear complicated to calculate, they are easily calculated in a computer worksheet. A Mathcad version is illustrated in Appendix A under the assumption that $\gamma_{tf} = \gamma_{cf} = 0.02,\ \beta_{sl} = 0.07$. Once the coefficients have been calculated, the elastic stress inequalities may be checked to provide bounds on the section properties. For example, to check the strength I limit state conditions, under the assumption that the resistance is limited to F_y, a pair of inequalities are written for the stress at the top and bottom of the steel section. These take the form

$$\phi F_y \geq \frac{\eta}{A_{tf} D}\left\{\frac{1.25M_{D_1}}{C_{T_{NC}}} + \frac{1.5M_{D_2} + 1.25M_{D_3}}{C_{T_{LT}}} + \frac{1.75[M_{La} + (1+I)M_{Tr}]}{C_{T_{ST}}}\right\}$$
$$\rightarrow A_{tf} \geq \frac{\eta}{\phi F_y D}\left\{\frac{1.25M_{D_1}}{C_{T_{NC}}} + \frac{1.5M_{D_2} + 1.25M_{D_3}}{C_{T_{LT}}} + \frac{1.75[M_{La} + (1+I)M_{Tr}]}{C_{T_{ST}}}\right\} \quad [14]$$

$$\phi F_y \geq \frac{\eta}{A_{tf} D}\left\{\frac{1.25M_{D_1}}{C_{B_{NC}}} + \frac{1.5M_{D_2} + 1.25M_{D_3}}{C_{B_{LT}}} + \frac{1.75[M_{La} + (1+I)M_{Tr}]}{C_{B_{ST}}}\right\}$$
$$\rightarrow A_{tf} \geq \frac{\eta}{\phi F_y D}\left\{\frac{1.25M_{D_1}}{C_{B_{NC}}} + \frac{1.5M_{D_2} + 1.25M_{D_3}}{C_{B_{LT}}} + \frac{1.75[M_{La} + (1+I)M_{Tr}]}{C_{B_{ST}}}\right\} \quad [15]$$

Equations [14] and [15] provide approximate bounds on the tension flange area A_{tf} as a function of *D*. The larger of the two bounds controls, and provided a reasonable starting estimate of A_{tf} for the assumed section dimension ratios in the current study. Subsequent revision of the α ratios provides rapid estimation of an economical section. The approach is also applicable to rolled sections with cover plates, provided the area A_{tf} is taken as the area of the flange *plus* the cover plate. If a subsequent revision of the beam section is needed based upon the serviceability II limit state, either the section currently being analyzed may be revised directly, or the comparable provision for serviceability limit state may be considered, and inequalities similar to those given above may be written.

Section Calculations to Estimate Girder Dimensions, Negative Bending:

For negative bending, it is also possible to rapidly estimate the size of efficient sections. In this case, the assumptions are that

1. Top and bottom flanges have equal area ($A_{cf} = A_{tf}$).
2. The web to compression flange ratio is given by $A_w \approx \alpha_w A_{cf}$.
3. The reinforcement to compression flange ratio is $A_R / A_{cf} = \alpha_R$. In the design calculations used in this project $A_R \approx 0.2 A_B$ was used as a first guess.
4. If *D* is the web depth, then the geometry of the section is *approximated* as shown in Figure 2.
5. The concrete is ignored in negative bending for strength purposes, although it may be considered for deflection calculations, according to AASHTO.

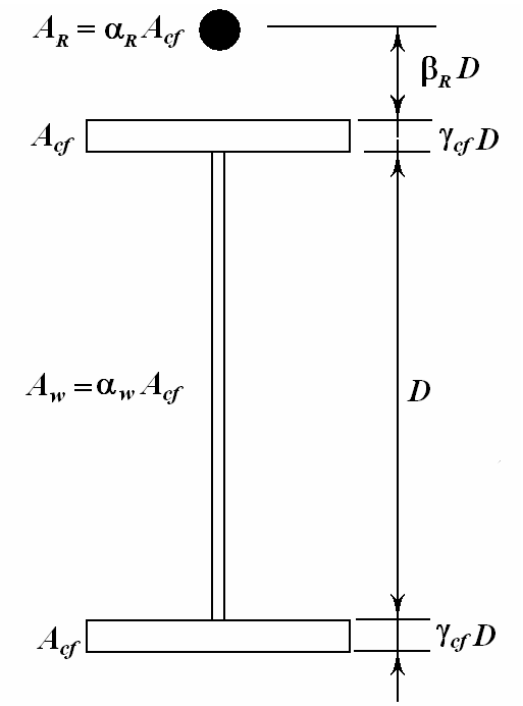

Figure 2. Cross-section properties for estimating minimum section requirements in negative bending

Then the non-composite elastic properties are

$$\begin{aligned} \bar{y}_B &= C_{0_{NC}} D \\ I_{NC} &= C_{1_{NC}} A_{cf} D^2 \\ S_{T_{NC}} &= S_{B_{NC}} = C_{T_{NC}} A_{cf} D \end{aligned} \qquad [16]$$

where

$$\begin{aligned} C_{0_{NC}} &= 0.5 + \gamma_{cf} \\ C_{1_{NC}} &= \frac{\alpha_w}{12} + \frac{\left(1+\gamma_{cf}\right)^2}{2} \\ C_{T_{NC}} &= \frac{C_{1_{NC}}}{C_{0_{NC}}} \end{aligned} \qquad [17]$$

Since the concrete is not effective at the failure limit state, it is not necessary to distinguish between long-term and short-term composite sections. Therefore, the composite section properties may be calculated as

$$\begin{aligned}
\Delta\bar{y}_B &= C_{0_C} D \\
I_C &= C_{1_C} A_{cf} D^2 \\
S_{T_C} &= C_{T_C} A_{cf} D \\
S_{B_C} &= C_{B_C} A_{cf} D
\end{aligned} \qquad [18]$$

where

$\Delta\bar{y}_B$ = the shift in the neutral axis under composite action

and

$$\begin{aligned}
C_{0_C} &= \frac{0.5 + \gamma_{cf} + \beta_R}{2 + \alpha_R + \alpha_w} \\
C_{1_C} &= C_{1_{NC}} + (2 + \alpha_w) C_{0_C}{}^2 + \alpha_R (0.5 + \gamma_{cf} + \beta_R - C_{0_C})^2 \\
C_{T_c} &= \frac{C_{1_C}}{C_{0_{NC}} - C_{0_C}} \\
C_{B_c} &= \frac{C_{1_C}}{C_{0_{NC}} + C_{0_C}}
\end{aligned} \qquad [19]$$

The plastic section properties are less likely to be relevant for negative bending, because of local and lateral stability issues, but can be estimated. For the composite section, the plastic neutral axis is located in the web at

$$\bar{d}_p = C_P D \qquad [20]$$

measured from the *top* of the compression flange. Typically, C_p will be between 0.5 and 0.6. Then the plastic section modulus may be estimated as

$$Z_C = C_z A_{cf} D \qquad [21]$$

In these calculations,

$$\begin{aligned}
C_p &= \frac{\alpha_w + \alpha_R \rho_y}{2\alpha_w} \\
C_z &= (C_p{}^2 - C_p + 0.5)\alpha_w + (1 + \gamma_{cf}) + (1 - C_p + \gamma_{cf} + \beta_R)\rho_y \alpha_R
\end{aligned} \qquad [22]$$

where $\rho_y = F_{y_R} / F_y$ is the ratio of the reinforcement yield strength to the steel plate yield strength. These equations are also valid if the section is designed in negative bending as if it were non-composite, except that in this case the reinforcement area would be taken as zero.

In a manner similar to that used for the positive section in bending, the negative bending coefficients for elastic and plastic section approximation are easily programmed in a worksheet for rapid calculation. A Mathcad worksheet is given in Appendix B for convenient reference.

Assuming that the negative section is limited to no more than F_y at the strength I limit state, it is relatively straightforward to obtain reasonable first estimates of section properties once the section properties are approximated as a function of A_{cf} and D. For negative bending, assuming that the maximum stress must not exceed F_y, these are given by

$$\begin{aligned} \phi F_y &\geq \frac{\eta}{A_{cf} D}\left\{\frac{1.25M_{D_1}}{C_{T_{NC}}} + \frac{1.5M_{D_2} + 1.25M_{D_3} + 1.75[M_{La} + (1+I)M_{Tr}]}{C_{T_C}}\right\} \\ \rightarrow A_{cf} &\geq \frac{\eta}{\phi F_y D}\left\{\frac{1.25M_{D_1}}{C_{T_{NC}}} + \frac{1.5M_{D_2} + 1.25M_{D_3} + 1.75[M_{La} + (1+I)M_{Tr}]}{C_{T_C}}\right\} \end{aligned} \quad [23]$$

$$\begin{aligned} \phi F_y &\geq \frac{\eta}{A_{cf} D}\left\{\frac{1.25M_{D_1}}{C_{B_{NC}}} + \frac{1.5M_{D_2} + 1.25M_{D_3} + 1.75[M_{La} + (1+I)M_{Tr}]}{C_{B_C}}\right\} \\ \rightarrow A_{cf} &\geq \frac{\eta}{\phi F_y D}\left\{\frac{1.25M_{D_1}}{C_{B_{NC}}} + \frac{1.5M_{D_2} + 1.25M_{D_3} + 1.75[M_{La} + (1+I)M_{Tr}]}{C_{B_C}}\right\} \end{aligned} \quad [24]$$

In a similar manner, if it were decided to attempt to design using the plastic section capacity, it is possible to write the inequality

$$A_{cf} \geq \frac{\eta\left[1.25M_{D_1} + 1.5M_{D_2} + 1.25M_{D_3} + 1.75\left(M_{La} + (1+I)M_{Tr}\right)\right]}{\phi C_Z F_y D} \quad [25]$$

It is easy to see from the coefficients calculated in the sample section design worksheet in Appendix B that the compression flange area estimated from the plastic section calculation is smaller than the area estimated from either of the elastic limit state equations. Therefore, in all cases, the plastic section area estimates will tend to be a lower bound on the feasible girder area for a given web depth, *D*.

Applying the Estimates:

In the current design studies, it was found adequate to simply use the estimation methods outlined above to obtain a first guess of flange and web areas for a given *D*. In the design of the 22.87 m bridges, rolled sections were used, and the area estimates were used to estimate the beam cross-sectional area and the cover plate size for a beam of the given depth that would result in areas comparable to those obtained from the first estimates. The resulting rolled beam section and cover plate were then used in the detailed design checks. Generally, it was found that very little resizing had to be employed to find a girder that was adequate, but economical.

The 45.73-m bridges and the multi-span bridge were designed using welded plate girders. For these bridges, the flange and web plate dimensions were obtained using the estimated flange and web areas, and the approximate dimensions were compared with the general section limits and the slenderness ratio limits on b_f / t_f and D / t_w. Since almost all of the lateral bending stiffness resides in the two flanges, the provision of AASHTO (1998), Section 6.10.2.1 may be written as

$$0.1 \le \frac{t_{cf} b_{cf}^{\ 3}}{t_{cf} b_{cf}^{\ 3} + t_{tf} b_{tf}^{\ 3}} \le 0.9 \qquad [26]$$

This requirement assures that the girder has a sufficiently large compression flange to behave as an I section. Generally, this requirement was easily satisfied with a flange area ratio $A_{cf} / A_{tf} \approx 0.5$. For negative bending, the provision is satisfied by observation, since the compression and tension flanges were taken as equal. The provision of section 6.10.2.2, was a bit more difficult to apply at an early stage, since the final value of D_c was not exactly known. In particular, the provision that

$$\frac{2D_c}{t_w} \le 6.77\sqrt{\frac{E}{f_c}} \le 200 \qquad [27]$$

must be considered at both the final composite stage, and at the non-composite stage. In positive bending, f_c takes its largest value, but D_c takes its smallest value in the final stage, under dead plus live load combinations. By contrast, in the non-composite stage, f_c is smaller, but D_c may take its largest value. In positive bending the non-composite value of D_c may be well over *D*/2. A conservative approach is to use the non-composite value of D_c together with the approximate stress $f_c \approx F_y$. However, failure to satisfy this approximate limit does not mean that the girder fails to satisfy the limit under the *actual* stress. By contrast, the largest value of D_c in negative bending regions is achieved in the composite state, where the stress is largest, so only one check needs to be conducted for that section. In a number of cases, a slight upward revision of web area resulted from checking the D / t_w limits. At this point, rather than conduct additional iterations against the approximate formulas given above, further checks were conducted using the estimated section dimensions against the design limit states.

Finally, the estimated compression flange widths were compared with the limits of section 6.10.3. Following these preliminary checks, the initial set of section dimensions were established, and the detailed check of provisions commenced. As a first step in this procedure, detailed section properties were calculated, using computer worksheets. Samples of these worksheets are given in Appendix C.

One variation from previous design codes should be noted. The concept of effective flange width is retained in the LRFD code. However, the formulae used to determine the effective widths differ slightly. For interior beams,

$$b_e = \min [\ L/4\ ,\ S\ ,\ 12t_s + \max(t_w,\ b_f/2)\ ] \qquad [28]$$

while, for exterior beams,

$$b_e = \min\ b_{eint}/2 + \min [\ L/8\ ,\ w_o\ ,\ 6t_s + \max(t_w,\ b_f/2)/2\ ] \qquad [29]$$

where L is the span length, S is the girder spacing, t_s is the interior slab thickness, w_o is the width of the deck overhang, t_w is the girder web thickness, and b_f is the girder flange width. In the current studies, the effective flange width definition update only affected the contribution of slab to the exterior girders.

Final Design Considerations

Once preliminary cross-section dimensions were obtained, the AASHTO design provisions were systematically checked. For the simple span bridges, the design calculations were based upon the moments at mid-span, which is the critical bending section both for final composite state moments, and for the construction stage stress calculations. Conditions checked included the strength I bending limit state, the serviceability II limit state, and the web fatigue limit state. The constructability limit state was used to adjust compression flange width if needed, or to adjust the distance between cross-frames to control lateral instability. The maximum shear was located at the ends, so the strength I shear stress limit state was used to determine the shear stiffener spacing requirements at the end of the beam.

The multi-span girder design was carried out in a similar fashion. The design began with the negative bending section, which tended to control the overall dimensions of the section. For the design carried out in this project, it was not found economical to design the negative bending section to be compact, both because of the need for extensive cross-frames to provide lateral stability, and because of web slenderness limitations that compactness imposes. It was found to be generally more efficient to design the girder as a non-compact girder with a relatively slender web, and with cross-frames at a larger spacing.

In a multi-span bridge, both shear and moment are large at the negative bending regions near the interior supports, so it was necessary to consider strength I, serviceability II, web shear strength, and interaction between web shear and bending resistance at the negative bending section. The lateral stability provisions of AASHTO (1998) for negative bending differ between the composite (tension flange supported against translation and rotation) and the pre-composite (tension flange *not* supported against translation and rotation) states. Therefore, separate consideration of lateral torsional buckling in the composite state and in the non-composite state is necessary at that section under LRFD.

After the negative section design was established, the positive section design was carried out as in the simply supported girder bridges, with one exception. Generally, the positive bending section is compact in the composite state, even with a relatively thin web, because the value of D_c tends to be small in the final limit state. The LRFD code does not specifically disallow using plastic design for positive bending together with stability based design for negative bending. Therefore it is, in principle, possible to design the positive bending section

using plastic capacity. However, in order to achieve M_p in the positive bending region, relatively large rotations must be possible at the mid-span, without loss of bending resistance at the supports. Stability considerations tend to control the design of the support regions, unless they are designed to be compact. Then large rotations in the support regions without loss of moment capacity are not assured. Since the support region will probably have to undergo large rotations in order to develop the large rotations at mid-span, it is non-conservative to design for plastic capacity at mid-span. Therefore, the section at mid-span was designed to limit maximum bending stresses to F_y under factored loads. This led to a slightly more conservative design. An alternative approach is to design the negative bending section to be compact. Then plastic design moments could be used for both positive and negative sections.

Strength in Bending

Generally, the Strength I limit state, given in eqn. [4] was checked first, to assure that the preliminary section was in adequate. A small amount of resizing was sometimes needed at this stage, but usually, the first estimates were surprisingly good. The nominal moment resistance M_n varies, depending upon whether the section is compact or non-compact. A section is specified as compact if it satisfies three different conditions: a web compactness criterion

$$\frac{2D_{cp}}{t_w} \le 3.76\sqrt{\frac{E}{F_{yc}}} \qquad [30]$$

a flange compactness criterion,

$$\frac{b_f}{2t_f} \le 0.382\sqrt{\frac{E}{F_{yc}}} \qquad [31]$$

and a lateral support criterion

$$L_b \le \left[0.124 - 0.0759\left(\frac{M_l}{M_p}\right)\right]\frac{r_y E}{F_{yc}} = L_{pd} \qquad [32]$$

In addition, a web-flange compactness interaction equation, not given here, must be considered.

Plastic Moment Capacity Calculation

All positive bending sections in the current project were compact in the final composite state. Therefore, some plastic capacity was nominally available, although as previously noted, it was not used for the multi-span girders. In order to use the plastic moment M_p as the positive bending capacity of a compact composite girder, it was first necessary to complete a ductility check to ensure that the rotations required to develop the plastic moment can occur without prior crushing of the slab (Wittry, 1993). First, the plastic neutral axis (PNA) was located and the plastic moment, M_p was found under the assumption that concrete crushing would not occur.

The ductility factor D_p/D' determines whether concrete crushing is a problem, where D_p is the distance from the top of the slab to the PNA, and D' is defined by

$$D' = \beta \frac{d + t_s + t_h}{7.5} \quad [33]$$

In equation [33], d is the overall depth of the steel girder, t_s is the thickness of the slab, t_h is the thickness of the haunch, and β is a parameter that depends upon the steel yield stress F_y. β equals 0.7 for steel with a yield stress of 345 MPa (50 ksi).

Once the ductility factor D_p/D' has been determined, the nominal moment capacity can be calculated. If $D_p/D' < 1$, then the nominal moment capacity is taken to be the full plastic moment, M_p. If $D' < D_p \le 5D'$, then the nominal moment resistance is calculated as:

$$M_n = \frac{5M_p - 0.85M_y}{4} + \frac{0.85M_y - M_p}{4}\left(\frac{D_p}{D'}\right) \quad [34]$$

where M_y is the moment capacity at first yield of the composite section. The yield moment M_y for the composite section is determined, as

$$M_y = M_{DC} + M_{DW} + M_{ADD} \quad [35]$$

M_{ADD} is the additional short-term composite moment required to bring the compressive stress to F_y and is the smaller of the values determined from the conditions that

$$\frac{M_{DC}}{S_{T_{NC}}} + \frac{M_{DW}}{S_{T_{LTC}}} + \frac{M_{ADD}}{S_{T_{STC}}} = F_y$$
$$\frac{M_{DC}}{S_{B_{NC}}} + \frac{M_{DW}}{S_{B_{LTC}}} + \frac{M_{ADD}}{S_{B_{STC}}} = F_y \quad [36]$$

Serviceability Limit States [6.10.5]

Following the Strength I bending resistance check, the Serviceability I and II provisions were checked. The serviceability limit states govern restrictions on stresses, deflections, and crack widths that occur under regular service conditions. Of the three serviceability limit states provided by AASHTO, Serviceability I and II apply to the bridges considered in this project. The serviceability I limit state is given by

$$\phi R \ge \eta \cdot \left[1.0(DC + DW) + 1.0(LL + IM) + 0.3(WS + WL)\right] \quad [37]$$

and the serviceability II limit state is

$$\phi R \ge \eta \cdot \left[1.0(DC + DW) + 1.3(LL + IM)\right] \quad [38]$$

In equations [37] and [38], the resistance factor ϕ and the load modifiers η are both equal to 1.0. The Serviceability I limit state relates to the normal operational use of the bridge with 90 km/h wind and with loads taken at their nominal values. The Serviceability II limit state relates only to steel structures and controls partial yielding due to vehicular live load, otherwise referred to as permanent deflection, or shakedown. In the Serviceability II limit state, the flange stresses for composite girders are limited to $0.95 F_y$. The design check for the Serviceability II permanent deflection criterion were carried out at top and bottom sections, as given by

$$0.95F_y \geq \frac{M_{DC}}{S_{Tnc}} + \frac{M_{DW}}{S_{Tlt}} + \frac{1.3M_{LL+IM}}{S_{Tst}}$$
$$0.95F_y \geq \frac{M_{DC}}{S_{Bnc}} + \frac{M_{DW}}{S_{Blt}} + \frac{1.3M_{LL+IM}}{S_{Bst}} \qquad [39]$$

The serviceability II provision controlled the design in several cases for the single span bridges, and some minor revision was necessary at this point. Serviceability II did not control the design of the multi-span girders, probably because the Strength I limit state stresses were already limited to F_y by the lack of negative bending ductility.

Construction Stresses Limit State

Following any cross-section modifications that were necessary as a result of the Strength I or Serviceability II provisions, the construction stage stresses were checked, and the diaphragm spacing was adjusted accordingly. In a couple of cases, minor adjustments of the compression flange dimensions were also introduced at this time.

During the construction phase, the steel girders supports the dead load *DC* (referred to in these calculations as D_1) that includes self-weight, the haunches, and the unhardened concrete slab. The limit state is the same as the other strength cases, except that only the non-composite dead load is considered, and the non-composite steel section provides the only resistance. The resulting construction limit state in bending is

$$\phi M_n \geq \eta \cdot (1.25M_{DC}) \qquad [40]$$

For the non-composite calculations, the redundancy factor η_r, of 0.95 should be used, since the structure is not laterally stiffened by the slab. This redundancy factor is one of three terms that define the load modifier η. Any available redundancy at this stage is provided by the lateral bracing, so great care should be taken to ensure that the lateral bracing is sufficient at construction loads. Because the compression flange is not laterally braced, and the neutral axis is located much lower in the section in the pre-composite stage, local and lateral stability conditions must be considered at this stage of design.

Strength in Shear [6.10.3 , 6.10.7]

After completing the flexural design of the section and checking for constructability, the shear Strength I provisions were used to determine the spacing of transverse stiffeners to ensure adequate shear resistance. In the current design studies, the shear design procedure followed was to first determine if the un-stiffened shear resistance was adequate to carry the load. If that calculation revealed that transverse stiffeners were needed, the resistance with the maximum permissible stiffener spacing for end and interior panels was evaluated. If that stiffener spacing was not adequate, a closer stiffener spacing was sought that would minimize the total number of stiffeners, but result in a sufficient resistance to satisfy the Strength I limit state for shear, which is given as

$$\phi V_n \geq \eta \cdot \left[1.25V_{DC} + 1.5V_{DW} + 1.75V_{LL+IM}\right] \qquad [41]$$

The relevant resistance factor is $\phi_v = 1$.

The shear resistance provisions in AASHTO (1998) are not substantially different from those in the ASD code, but the notation has been changed to make the code more independent of the system of units. Therefore, detailed discussion of the shear provisions is omitted. Interested readers may refer to Simons (2005) for further details.

Fatigue and Fracture Limit State

In the current design project, the girders were not fully detailed, so only limited checks of detail fatigue were conducted to assure that the designs were capable of achieving the desired number of load cycles.

The fatigue and fracture limit state governs restrictions on stress range caused by a design fatigue truck. The provision is intended to limit crack growth under repetitive loads and prevent fracture due to shakedown, or cumulative stress effects in steel elements. The fatigue limit state is

$$U = \eta \cdot \left[0.75\left(LL + IM\right)_F\right] \qquad [42]$$

In eqn. [42] the subscript *F* implies that the fatigue truck is used. Since the vehicular live load is the only load that causes a large number of repetitive cycles, it is the only loading that is considered for fatigue of details. However, the majority of trucks do not exceed the legal weight limit, so to use the full vehicular live load would be unduly conservative. Therefore a less severe live load model is used, a single design truck with the variable axle spacing set to 9 m. It should also be noted that for the fatigue provision, a dynamic load allowance of 15% is used rather than the 33% used in most other limit states. Additionally a load factor of 0.75 is applied to this live load and its associated impact factor, since the average load effect of survey vehicles was about 75% of the moment due to the design fatigue truck (Nowak 1993). Other than a change in the loads to be applied at the fatigue limit state, and a change from tabulated numerical values to equations for fatigue resistance, the provisions for fatigue are relatively similar to the AASHTO ASD provisions, so they are not discussed further.

Web Bend Buckling Fatigue

Web bend buckling considerations were of somewhat greater importance in the current project than detail fatigue considerations, since they had some influence upon the minimum usable web thickness in a couple of cases. This was particularly true in the negative bending regions. These provisions were checked after the strength I bending limit state check, since the relevant moments and section properties were readily available at that time. The LRFD provisions represent a significant change from ASD practice, so some further discussion is warranted.

In current design practice, the use of plate girders with transverse stiffeners may lead to relatively thin webs that are susceptible to bend buckling. AASHTO (1998) provisions are less restrictive on web thickness than AASHTO (2002), exacerbating this situation. Specifically, at the Strength I limit state, the compression portion of the web may be in a buckled state, provided the "load shedding" of stress to the compression flange, and the resulting decrease of strength are properly taken into account. However, studies have shown that the web bending must be limited under service level loads to prevent the development of fatigue cracks (Yen and Mueller, 1966; Mueller and Yen, 1968). Web bending buckling occurs as a result of the combined action of dead and live loads, so the total bending stress in the web must be limited, not just the live load stress range. To control the web normal stress that may lead to web buckling, the maximum elastic stress is limited by the web buckling stress.

According to Barker and Puckett (1997), "the flexural web buckling stress is based on elastic plate buckling formulas with partially restrained edges." The first edition of AASHTO LRFD defined a web slenderness ratio, $\lambda_w = \frac{2D_c}{t_w}$, to help define the web buckling capacity. In the second edition, this ratio was replaced with the simpler ratio D/t_w, but the equations for the limiting flange compression stresses were modified accordingly. For webs without longitudinal stiffeners, the maximum flexural stress in the compression flange f_{cf}, which is representative of the maximum bending stress in the web, is limited by

$$f_{cf} \le \begin{cases} F_{yw} & \text{if } D/t_w \le 0.95\sqrt{kE/F_{yw}} \\ 0.9kE(t_w/D) & \text{if } D/t_w > 0.95\sqrt{kE/F_{yw}} \end{cases} \qquad [43]$$

The factor k is defined, for webs without longitudinal stiffeners as:

$$k = 9\left(\frac{D}{D_c}\right)^2 \ge 7.2 \qquad [44]$$

In the resulting equations for f_{cf}, the variable R is hybrid flange stress reduction factor, and for homogeneous sections considered in the current study the value is equal to 1.0.

In the AASHTO ASD specification, web bend buckling was prevented through a limit on the ratio D/t_w. The AASHTO LRFD provision recognizes the variation in the location of the

neutral axis relative to the mid-height of the web, so the ratio $2D_c / t_w$ is used instead. In the first edition of AASHTO LRFD, this was accomplished through the explicit inclusion of D_c in all of the limiting equations. In the second edition, this is accomplished indirectly through the use of the factor *k*. Using the depth of compression in the web adds another degree of sophistication to the design process. The result is a more accurate model of web behavior, and a less conservative provision than provided by ASD.

The web fatigue provision is carried out using the fatigue load combination, except that the fatigue truck load is doubled, leading to the load combination

$$\phi f_{cf} \geq \frac{M_{DC}}{S_{T_{NC}}} + \frac{M_{DW}}{S_{T_{LTC}}} + 0.75\frac{(1+IM_{Fatigue})(2M_{FT})}{S_{T_{STC}}} \qquad [45]$$

In both the detail fatigue and web bend buckling fatigue provisions, the fatigue truck moment M_{FT} is distributed to the girders using a distribution factor for a single vehicle crossing. Therefore the 1.2 multipresence factor is to be excluded. AASHTO LRFD does not discuss this matter, but if the multipresence factors have automatically been included, as in analysis using distribution factors, the resulting distributed moment should be divided by 1.2. Generally, this check did not control the designs carried out in the present study, except in the negative bending regions of the multi-span girder. Typically, D_c was relatively small in positive bending regions, and other limits tended to control the web dimensions in the negative bending regions.

Diaphragms and Cross Frames

For the current project, the cross frames are composed of angles bolted to plates, which are in turn welded to the web of the connected girders. Similar to the ASD code, the LRFD code requires that the cross frames must be designed to withstand the force effect of a 2.394 kPa (50 lbs/ft^2) wind load applied to the exposed elevation of the bridge, but not less than 407 kN/m (300 lb/ft) along the bridge. In the current designs, cross frame locations were chosen as a fraction of the span length based upon consideration of both lateral stability and wind induced lateral bending stresses in the tension flange. Generally, it was found that the stresses in the cross-frame members were small, with minimum dimensions being controlled by slenderness limits, and the sizes of available sections. One significant change from ASD to LRFD is the maximum spacing of diaphragms or cross-frames. Under the ASD specification, maximum spacing of diaphragms is 25 ft (7.6 m). However, cross-frame and diaphragm locations have been found to be a source of fatigue cracking, and the benefits of diaphragms in increasing interaction between girders has been found to be somewhat limited. Therefore the prevailing current philosophy, implemented in the LRFD specification, is to maximize cross-frame or diaphragm spacing, consistent with lateral stability, and wind loading requirements. In the current project, this typically led to a larger spacing of cross-frames in the LRFD designs, with occasional need for temporary bracing during construction.

Lateral Stability Design Considerations

In the design studies carried out for this project, lateral stability considerations presented one of the major complicating factors in the design process. Lateral stability tended to control the spacing of the cross-frames in a number of cases. In most cases, proper spacing of the cross-frames allowed the provisions to be satisfied without significant revision of compression flange dimensions. However, from a strict economy viewpoint, if it is desired to minimize the number of cross frames, as recommended by AASHTO, increasing compression flange width may be a reasonable design approach.

The lateral stability considerations in the LRFD specification (AASHTO, 1998) are significantly more complex than those in the ASD specifications (AASHTO, 2002) so the interpretation of these specifications for the current project is presented in some detail. The compression flange of a composite section in positive bending receives continuous lateral support from the concrete slab. Therefore, in the final composite state, lateral stability of sections in positive bending is not an issue. However, lateral stability may be a limiting factor in the resistance of a steel girder under several different conditions. These include

(a) Composite construction is not used. Although it has been found in practice that slabs continue to provide some lateral support even though non-composite construction is used, that lateral support is not dependable, so the girder must be designed as if the slab provides negligible lateral support. An exception to this limitation would occur if the haunches are extended beyond the flange edges by a reasonable amount and "wrap" the flanges. Then lateral support could be assumed. The bridges for the current project were all composite, so this situation was not encountered.

(b) Composite construction is used, but the girder is in the non-composite state. The heaviest load to be expected on the girder before composite action becomes effective is the combined weight of the girder and diaphragm system, together with the wet, non-composite slab. This case governed the behavior of the non-composite structure in both positive and bending regions.

(c) Composite action is effective, with the top flange embedded in the concrete haunch, but the section is in negative bending, so the compression flange is not continuously laterally braced. This situation is encountered in the negative bending regions of a composite beam.

AASHTO LRFD provides two distinct lateral-torsional buckling provisions to accommodate these three possibilities. The first provision is intended to prevent lateral torsional instability for sections whose tension flange is free to rotate, and is given in AASHTO section 6.10.4.2.6. This provision covers cases (a) and (b). The second provision is intended to prevent lateral torsional instability for sections whose tension flange is restrained from rotation by the composite action of the slab and is given in section 6.10.4.2.5. This covers case (c). Although it is possible that a non-composite slab that wraps the tension flange would also restrain tension flange rotation, it is more conservative to neglect this restraint for all non-composite behavior.

Sections Not Subject to Lateral Torsional Instability

AASHTO recognizes two distinct classes of sections not subject to lateral torsional instability, depending upon whether the flange and web are compact or not.

(a) If the compression flange and web satisfy the local compactness requirements given by equations [30]-[32] or if the section is continuously supported by a composite slab, then the section is compact, and the limiting resistance is given by eqn. [34]. Such sections have full lateral support. The length limit specified in this equation corresponds to the length L_{pd} in the AISC specification, (AISC, 2001), which according to Salmon and Johnson (1996) is an unbraced length that permits development of M_p, *plus* large plastic rotations. Both AASHTO and AISC specifications permit the use of plastic redistribution of moments for girders satisfying the web and flange compactness provisions, together with this maximum unbraced length requirement. AASHTO (1998) does not use the terminology L_{pd}, but it is convenient to use that terminology in the remainder of the present discussion.

(b) If a section does not satisfy the above lateral bracing requirement, AASHTO (1998) refers to it as *non-compact*, even if the flange and web satisfy all width-thickness ratio limits for compactness. Alternately, even if the compression flange is supported along its entire length, but does not satisfy the web width-thickness compactness ratio limits, the girder is said to be non-compact. If the unbraced length satisfies the condition

$$L_b \le L_p = 1.76 r_t \sqrt{\frac{E}{F_{yc}}} \qquad [46]$$

then, AASHTO (1998) assumes that the section has sufficient lateral bracing to be capable of reaching the yield stress in the compression flange before the onset of lateral instability. AASHTO then considers two possibilities, depending upon whether local instability of web or flange can occur prior to compression flange yielding. Readers familiar with the AISC LRFD design specifications will recognize that L_{pd} satisfies the relationship $L_{pd} < L_p$. AASHTO LRFD's interpretation is more conservative than AISC's, limiting maximum flange stress at the extreme fiber to no more than F_{yc}, which in essence limits the maximum moment to M_y. By contrast, AISC continues to allow sections with compact web and flange properties to carry M_p if $L_{pd} < L_b < L_p$, but does not allow redistribution of moment.

A composite section in positive flexure in the final condition cannot undergo flange instability before yielding, even if web and flange are non-compact, because the slab prevents local flange buckling, so the limiting stress for such sections is

$$F_n = R_b R_h F_{yc} \qquad [47]$$

where R_h is a hybrid section stress reduction factor that accounts for the possibility that the web may yield prior to flange yielding, with a resultant transfer of stress to the compression flange if $F_{yw} < F_{yc}$, and R_b is the load shedding factor, intended to account for the increase in flange stress that accompanies bend buckling of the web at the strength limit state. R_h and R_b will be discussed subsequently. Calculation of L_b limits are not relevant for a composite section in positive bending in the final state.

For non-compact sections with an unbraced length $L_{pd} < L_b < L_p$, local flange buckling could initiate failure at a flange stress lower than F_y, so AASHTO limits the stress to

$$F_n = R_b R_h F_{cr} \qquad [48]$$

where F_{cr} is the local flange buckling stress. If the web is not stiffened longitudinally, AASHTO LRFD gives the local flange buckling stress as

$$F_{cr} = \frac{1.904E}{\left(\frac{b_f}{2t_f}\right)^2 \sqrt{\frac{2D_c}{t_w}}} \le F_{yc} \qquad [49]$$

The presence of the web aspect ratio $2D_c / t_w$ reflects the resistance of the web to rotation as the flange buckles. If longitudinal stiffeners are provided, the web has greater resistance to rotation, and the critical flange local buckling stress is given as

$$F_{cr} = \frac{0.166E}{\left(\frac{b_f}{2t_f}\right)^2} \le F_{yc} \qquad [50]$$

Although the second equation is based upon a larger dependable rotation restraint, the first equation will actually predict a larger critical stress value if $2D_c / t_w < 131.5$.

Sections Subject to Lateral Torsional Instability

Sections for which $L_b > L_p$ are subject to lateral torsional instability before flange yielding. AASHTO has two distinct provisions to handle this case, consistent with the fact that girders have both non-composite and composite behavior during their design life.

For composite girders, in their final condition, the top flange is connected to the slab. This precludes lateral buckling, or local flange buckling in regions of positive moment. Lateral instability in regions of negative bending may still be a problem. For negative moment regions of composite girders, lateral instability remains a possibility. The tension flange is not able to

rotate, being embedded in the slab, so it will provide some rotational resistance, and an enhanced lateral torsional buckling strength. AASHTO LRFD, section 6.10.4.5 defines two regions of behavior, depending upon the ratio

$$L_r = 4.44 r_t \sqrt{\frac{E}{F_{yc}}} \qquad [51]$$

If $L_p < L_b \le L_r$, inelastic lateral torsional buckling may occur, leading to a nominal resistance

$$F_n = C_b R_b R_h F_{yc} \left[1.33 - 0.87 \frac{L_b}{r_t} \sqrt{\frac{F_{yc}}{E}} \right] \le R_b R_h F_{yc} \qquad [52]$$

while if $L_b > L_r$, elastic lateral torsional instability must be considered with a nominal resistance

$$F_n = C_b R_b R_h \left[\frac{9.86E}{\left(L_b / r_t \right)^2} \right] \le R_b R_h F_{yc} \qquad [53]$$

In both equations, the modifier

$$C_b = 1.75 - 1.05 \frac{P_l}{P_h} + 0.3 \left(\frac{P_l}{P_h} \right)^2 \le K_b \qquad [54]$$

accounts for the beneficial effect of moment gradient. Because of the complexity of dealing directly with the moment in a composite girder, with multiple stages of loading, this provision, which is similar to the traditional AISC equation, has been rewritten in terms of the compression flange forces instead of the moments. The AASHTO (1998) commentary also permits the newer expression for C_b that was introduced by AISC (1993) but written in terms of flange compression forces as

$$C_b = \frac{12.5 P_{\max}}{2.5 P_{\max} + 3P_A + 4P_B + 3P_c} \qquad [55]$$

to be used in regions of non-linear moment gradient between brace points.

For non-composite girders, or girders in their non-composite state, in both positive and negative bending regions, the tension flange is assumed to be free to rotate, so it cannot provide resistance to rotation of the compression flange during lateral torsional buckling. Then AASHTO LRFD 6.10.4.2.6 provisions must be used. The nominal resistance is expressed in terms of moment, rather than stress, since the complication associated with the multiple stages of

construction in composite girders is not present. Two regions of behavior are recognized, depending upon whether the web is likely to undergo bend buckling before the commencement of lateral torsional buckling. Web bend buckling is not likely to precede lateral torsional buckling if either

- A longitudinal stiffener is provided, *or*
- The web compression zone satisfies the relationship.

$$\frac{2D_c}{t_w} \le \lambda_b \sqrt{\frac{E}{F_{yc}}} \qquad [56]$$

In this case, no reduction for web bend buckling needs to be considered, and the lateral torsional buckling limit is

$$M_n = 3.14EC_bR_h \frac{I_{yc}}{L_b} \sqrt{0.772\left(\frac{J}{I_{yc}}\right) + 9.87\left(\frac{d}{L_b}\right)^2} \le R_h M_y \qquad [57]$$

where I_{yc} is the moment of inertia of the compression flange about the vertical (web) direction, J is the St. Venant torsion constant for the section, and d is the overall depth of the section.

If the web is *not* longitudinally stiffened, and $\frac{2D_c}{t_w} > \lambda_b \sqrt{\frac{E}{F_{yc}}}$, then web bend buckling is expected to reduce the resistance. In this case, the nominal moment resistance is given in two parts. The length L_r is now given by the modified equation

$$L_r = 4.44 \sqrt{\frac{I_{yc} d}{S_{xc}} \frac{E}{F_{yc}}} \qquad [58]$$

where S_{xc} is the section modulus of the compression flange about the horizontal axis. If $L_p < L_b \le L_r$, the inelastic lateral torsional buckling equation is

$$M_n = C_bR_bR_hM_y \left[1 - 0.5\left(\frac{L_b - L_p}{L_r - L_p}\right)\right] \le R_bR_hM_y \qquad [59]$$

The inelastic lateral torsional buckling equation is obviously a linear interpolation between $C_bR_bR_hM_y$ and $0.5C_bR_bR_hM_y$. If $L_b > L_r$, elastic lateral torsional buckling must be considered, with a nominal resistance given by

$$M_n = C_b R_b R_h \frac{M_y}{2}\left(\frac{L_r}{L_b}\right)^2 \le R_b R_h M_y \qquad [60]$$

For non-composite girders, it is simpler, and equivalent, to express the moment gradient correction C_b directly in terms of the moments, rather than in terms of the compression flange forces. In either case (a) or (b), the nominal stress that can be used is the smaller of the lateral buckling stress, or the local buckling stress. Therefore, if the compression flange is subject to both lateral torsional buckling and local flange buckling, the limit that is reached first governs the design of the beam.

Flange Stress Reduction Factors

The flange stress reduction factors R_h and R_b account for a loss of elastic load carrying capacity by the compression part of the web, with a resulting increase in the compression flange stress. These also reflect a significant increase in sophistication relative to the ASD specification and deserve discussion. These factors may enter the calculations under two circumstances.

Although hybrid girders are not considered in present study, a brief discussion of the hybrid stress reduction factor R_h is included for completeness. If the yield stress of the web steel is lower than the yield stress of the compression and tension flanges, partial yielding of the web may occur, leading to an increase in the compression flange stress relative to that predicted by elastic beam theory for a given moment. AASHTO (1998) determines this effect by using the factor R_h. The function to be used to estimate R_h depends upon the state of the beam. AASHTO LRFD provides three different cases.

Case 1: Composite hybrid section positive bending: The neutral axis will be high in the section with yielding most likely to occur in the tension region of the web adjacent to the tension flange. Then R_h is calculated as

$$R_h = 1 - \left[\frac{\beta\psi(1-\rho)^2(3-\psi+\rho\psi)}{6+\beta\psi(3-\psi)}\right] \qquad [61]$$

where $\rho = \dfrac{F_{yw}}{F_{yb}} = \dfrac{\text{yield stress of web}}{\text{yield stress of bottom flange}}$

$$\psi = \frac{d_n}{d} = \frac{\text{distance from bottom flange extreme fiber to NA}}{\text{depth of steel section}}$$

$$\beta = \frac{A_w}{A_{fb}} = \frac{\text{area of web}}{\text{area of bottom flange}}$$

Case 2: Noncomposite sections where $|D/2 - D_c| \le 0.1D$. For these sections, the neutral axis is near mid-height of the beam, so the section may be approximately represented as doubly symmetrical. Then

$$R_h = \frac{12 + \beta(3\rho - \rho^3)}{12 + 2\beta} \qquad [62]$$

where

$$\rho = \frac{F_{yw}}{f_{fl}} = \frac{\text{web yield stress}}{\text{minimum of flange yield stress or stress due to factored loading}} \le 1$$

$$\beta = \frac{2A_w}{A_{tf}} = \frac{2(\text{web area})}{\text{sum of top and bottom flange areas}}$$

Case 3: Non-composite sections where $| D/2 - D_c | > 0.1D$. These sections cannot be approximated as doubly symmetrical. Then

$$R_h = \frac{M_{yr}}{M_y} = \frac{\text{yield moment for which web yielding is accounted}}{\text{yield moment disregarding web yielding}} \qquad [63]$$

The AASHTO (1998) commentary provides an approximate method for evaluating R_h in this case.

If the web is slender, it may undergo bend buckling, leading to a decrease of web contribution to the moment resistance. This loss of effective strength is introduced through the load shedding factor R_b. If the web is sufficiently thick, or if longitudinal stiffeners are provided, web bend buckling will not occur before yielding and $R_b = 1$. This will occur if either a web without longitudinal stiffeners satisfies

$$\frac{2D_c}{t_w} \le \lambda_b \sqrt{\frac{E}{f_c}} \qquad [64]$$

or a web with one or two longitudinal stiffeners satisfies

$$\frac{D}{t_w} \le 1.01 \sqrt{\frac{Ek}{f_c}} \qquad [65]$$

In the above, f_c is the compression stress at the extreme fiber under factored loadings, λ_b is a factor specified by section 6.10.4.3.2.a, depending upon the depth of the compression zone, and *k* is a factor that reflects the bend buckling resistance of the web. When the applicable ratio is exceeded, web bend buckling does occur, and the load shedding factor is given by

$$R_b = 1 - \left(\frac{a_r}{1200 + 300a_r} \right) \left(\frac{2D_c}{t_w} - \lambda_b \sqrt{\frac{E}{f_c}} \right) \qquad [66]$$

This factor is based upon fundamental studies by Basler (1961). In the equation,

$$a_r = \frac{2D_c t_w}{A_c} \quad [67]$$

where A_c is the area of the compression flange.

RESULTS

General

Since AASHTO's change from ASD to LRFD highway bridge design specifications involves changes in loads, analysis, and resistance provisions, a comparison of the two codes can be conducted on many different levels. The current study attempts to focus on aspects of the design codes that control a bridge's girder dimensions, flexibility, and dynamic characteristics. The results of this study include a comparison of the two load modeling and application methods, an analysis of the final girder designs for each of the 12 simple spans and the two multispan bridges considered, and a deflection analysis of the single span bridge designs. An investigation of the dynamic characteristics of these bridge superstructures as modeled with finite elements is presented in a separate report (Baber and Simons, 2005). The intent of the comparisons of the AASHTO ASD and LRFD methods and the structures they produce is to provide engineers with a better understanding of AASHTO's implementation of LRFD philosophies, and the changes that may be expected in designs as a result.

Load Modeling and Application

Three of the more significant changes in the AASHTO specifications involve the vehicular live load models, the impact factors or dynamic load allowance, and the distribution factors. The background of these revisions were discussed in the introduction. The following sections examine the results of applying these procedures to the bridge designs conducted in the current study. To provide insight into the overall effect of these individual changes, the final design live load moments and shears are examined as well.

Vehicular Live Loads

The vehicular live loads and dead loads are typically the most significant loads applied to highway bridge superstructures. Other loads may play a dominant role in design of substructures but are not of equal importance in the superstructure designs considered for the present study. Dead load models have not changed significantly, but substantial changes in live load model and application procedures may have a pronounced effect upon the design. Simons (2005) has provided a detailed discussion.

As discussed in the Introduction, the major changes in live load models introduced in moving from the AASHTO ASD specification to the AASHTO LRFD specification consists of the following:

(a) The alternative application of the HS-20 truck loading or the lane loading plus concentrated load has been replaced by a combination of the HS-20 truck loading together with the lane loading.
(b) The concentrated loads previously associated with the lane loading have been eliminated.
(c) A more precise definition of the fatigue truck loading has been given.

Detailed comparison of the moments and shears resulting from these changes is not particularly meaningful by itself, since the AASHTO ASD loadings are applied in an elastic (unfactored) manner, while the LRFD loadings are multiplied by the strength, serviceability, and fatigue limit state factors. However, following the rationale used in developing the HL-93 loading, it is anticipated that the unfactored HL-93 moments and shear will be somewhat larger than the HS-20 values.

Dynamic Loading Effects

As discussed by Simons (2005), dynamic loading effects are influenced by numerous characteristics of the bridge and vehicles, and the likelihood of the maximum load and impact coinciding. This behavior is complicated to model analytically, and the engineering community has not reached a consensus on the best method. The AASHTO ASD code provides an impact factor defined by a relationship that considers the length of the bridge span. The AASHTO LRFD code simplifies the behavior further and provides constant dynamic load allowances. For additional comparison, the 1983 Ontario Highway Bridge Design Code provided impact factors based upon the natural frequency of the bridge, but this approach was abandoned due to the difficulty in obtaining a reasonably accurate estimate of the frequencies before the design was completed. In 1993, the OHBDC thus chose constant dynamic load allowances based upon the number of axles included in the loading. Although the OHBDC is not directly relevant for practice in the United States, that code has been regarded as a relatively progressive code, so it is useful to include for comparison with ASD and LRFD codes. After reviewing each of these methods, a comparison was made of the impact factors and dynamic load allowance as they apply to the 12 bridges considered in this study loaded with one or two axles at a time. The results of this comparison for each span length are included in Table 1. A comparison of the ASD and LRFD factors for the multi-span bridge is shown in Table 2.

	ASD	LRFD	OHBDC 1983	OHBDC 1993
22.86 m	0.25	0.33*	0.4	0.3 - 0.4
45.72 m	0.18	0.33*	0.34 - 0.4	0.3 - 0.4

Table 1. Impact factors and dynamic load allowances- Simple Span Bridges

Girder Location	ASD (1+I)	LRFD (1+I)	LRFD (1+I) / ASD (1+I)
100	1.22	1.33	1.09
104	1.22	1.33	1.09
110,200	1.2	1.33	1.11
205	1.17	1.33	1.14

Table 2. Impact Factors and Dynamic Load Allowances - Multispan Bridge

Based upon the tabulated values, it is apparent that the ASD impact factors will predict a smaller dynamic effect than each of the other three methods. The amount of increase to be expected in design moments solely as a result of the change from ASD impact factors to LRFD dynamic load allowances is shown in the final column of Table 2 for the multi-span bridge. The girder locations given in Table 2 refer to span 1 (end span) or 2 (center span). The spans are then divided into ten equal length segments, and the stations on the span are denoted from 00 (left end) to 10 (right end). Therefore station 104 is 40% of the distance from the left end of span 1, 205 is the middle of span 2, and so forth.

In fact, the percentage increases shown in Tables 1 and 2 overstate the increase in design live load moments and shears resulting from the multiplier (1+*I*), since the factor *I* is applied to the total applicable live load in the ASD specification, but is only applied to the truck load moments and shears in LRFD, and not to the additive lane loading. Therefore, the effective increase in impact factors when applied to the total live load is either relatively small, or may reflect an actual decrease when the total live load is taken into account.

It is interesting to note that the LRFD dynamic load allowances correlate fairly well with both OHBDC methods. This suggests that the AASHTO LRFD method provides a reasonable value for *IM* while eliminating the complicated analyses required by OHBDC 1983. As noted above, however, not only the numerical value of the factor, but also the load to which it is applied must be considered in comparing dynamic amplification effects.

Distribution Factors

The AASHTO ASD (AASHTO, 2002) and LRFD (AASHTO, 1998) specifications both provide distribution factor methods for use in transferring live loads from the slab to each individual girder. The dependent variables for the two methods differ greatly. The ASD distribution factors depend solely upon the girder spacing, while the LRFD factors consider span length, girder stiffness, and multiple presence as well. In addition, the ASD code applies the same distribution factors for moments and shears, while the LRFD code has two sets depending on the type of response being calculated. Zokaie (1991) indicates that using the LRFD distribution factors produces results that are within 5% of the results found in finite element deck analysis for a fairly wide range of bridge parameters.

The distribution factors for moment and shear used for each of the twelve simple span bridges considered in this study are listed in Tables 3 and 4, and the distribution factors used for the three span continuous bridges are listed in Tables 5 and 6. In Tables 5 and 6, the girder locations are defined as described above for Table 2, and the suffixes I and E refer to interior or exterior girders.

	22.86 m - ASD		22.86 m - LRFD		45.72 m - ASD		45.72 m - LRFD	
	int	ext	int	ext	int	ext	int	ext
6 Girders	0.73	0.667	0.651	0.762	0.73	0.667	0.577	0.762
5 Girders	0.915	0.769	0.764	0.849	0.915	0.769	0.674	0.849
4 Girders	1.22	0.914	0.942	0.942	1.22	0.914	0.83	0.937

Table 3: Distribution factors for moment - Single Span Bridges

	22.86 m - ASD		22.86 m - LRFD		45.72 m - ASD		45.72 m - LRFD	
	int	ext	int	ext	int	ext	int	ext
6 Girders	0.73	0.667	0.826	0.726	0.73	0.667	0.826	0.762
5 Girders	0.915	0.769	0.966	0.849	0.915	0.769	0.966	0.849
4 Girders	1.22	0.914	1.185	0.952	1.22	0.914	1.185	0.952

Table 4: Distribution factors for shear- Single Span Bridges

Girder Location	ASD	LRFD	LRFD / ASD
M104I	0.67	0.621	0.927
M110I,M200I	0.67	0.590	0.881
M205I	0.67	0.568	0.848
ME	0.635	0.762	1.20

Table 5. Distribution factors for moments - Multi-span Bridge

Girder Location	ASD	LRFD	LRFD / ASD
V100I	0.67	0.826	1.23
V110I	0.67	0.826	1.23
V200I	0.67	0.826	1.23
VE	0.635	0.726	1.14

Table 6. Distribution factors for shears - Multi-span Bridge

The ASD distribution factors are calculated using the wheel line, or half the axle weight. Therefore the calculated ASD distribution factors are on the order of twice the value of the LRFD distribution factors. In order to facilitate a comparison of the two sets of values, the ASD factors presented in the preceding tables are adjusted to represent the full axle weight. It is also important to note that the ASD distribution factors are the same for both moment and shear, while the LRFD factors use different relationships for each response quantity.

A consistent relationship between the ASD and LRFD factors is not immediately evident. When these factors are presented as ratios, they are easier to compare. Tables 7 and 8 include ratios of the LRFD distribution factors to the corresponding ASD factors for both moment and shear for the twelve single span bridges, while the ratios for the multi-span bridge are given in the last column of Tables 5 and 6.

	22.86 m		45.72 m	
	int	ext	int	ext
6 Girders	0.892	1.142	0.790	1.142
5 Girders	0.835	1.104	0.737	1.104
4 Girders	0.772	1.031	0.680	1.025

Table 7: Ratios of LRFD to ASD moment distribution factors (LRFD / ASD)- Single Span Bridges

	22.86 m		45.72 m	
	int	ext	int	ext
6 Girders	1.132	1.088	1.132	1.142
5 Girders	1.056	1.104	1.056	1.104
4 Girders	0.971	1.042	0.971	1.042

Table 8: Ratios of LRFD to ASD shear distribution factors (LRFD / ASD) - Single Span Bridges

Design Moments and Shears

The AASHTO LRFD code has introduced numerous changes to the AASHTO live load modeling techniques. All of these changes were made in an attempt to produce a more accurate model of live load response in girders. The net effect of changes in live load models, impact factors, and distribution factors cannot fully understood until the final live load design moments and shears, including the effect of distribution factors and dynamic load allowances are calculated. The resulting design loads for the six pairs of simple span bridge designs are presented in Tables 9 and 10.

	22.86 m - ASD		22.86 m - LRFD		45.72 m - ASD		45.72 m - LRFD	
	int	ext	int	ext	int	ext	int	ext
6 Girders	1350	1233	1676	1962	2881	2633	3965	5236
5 Girders	1692	1422	1967	2186	3610	3036	4631	5833
4 Girders	2255	1689	2426	2426	4818	3609	5702	6438

Table 9: Live load design moments (kN-m) - Simple Span Bridges

	22.86 m - ASD		22.86 m - LRFD		45.72 m - ASD		45.72 m - LRFD	
	int	ext	int	ext	int	ext	int	ext
6 Girders	267	237	400	369	269	259	510	470
5 Girders	344	273	468	411	346	298	596	524
4 Girders	463	325	574	461	465	352	731	587

Table 10: Live load design shears (kN) - Simple Span Bridges

The LRFD code produced higher design moments and shears in every bridge design case considered in this study. This can be seen more clearly in Table 11, which includes the ratios of the unfactored LRFD design moments and shears to the ASD design moments and shears.

	LRFD M_{LL+IM} / ASD M_{LL+IM}				LRFD V_{LL+IM} / ASD V_{LL+IM}			
	22.86 m		45.72 m		22.86 m		45.72 m	
	int	ext	int	ext	int	ext	int	ext
6 Girders	1.24	1.59	1.38	1.99	1.50	1.56	1.90	1.81
5 Girders	1.16	1.54	1.28	1.92	1.36	1.51	1.72	1.76
4 Girders	1.08	1.44	1.18	1.78	1.24	1.42	1.57	1.67

Table 11: Ratios of unfactored LRFD live load moments and shears to ASD live load moments and shears - Single span bridges

A similar conclusion is reached for the moments and shears in the pair of multi-span bridges, as shown in Table 12. The moments and shears to be applied in LRFD design are consistently at least 41% larger than those for ASD, and several of the exterior girder values are more than 100% larger.

Location, Quantity	ASD Interior L(1+I)	LRFD Interior L(1+I)	Int. LRFD / Int. ASD	ASD Exterior L(1+I)	LRFD Exterior L(1+I)	Ext. LRFD / Ext. ASD
Moments (kN-m) and Moment Ratios						
M104	1371 (Tr)	1936	1.41	1299 (Tr)	2375	1.83
M200	-1927 (La)	-2833	1.47	-1826 (La)	-3659	2.00
M205	1762 (Tr)	2709	1.54	1670 (Tr)	3437	2.06
Shears (kN) and Shear Ratios						
V100	293 (Tr)	422	1.44	287 (Tr)	390	1.36
V110	-293 (La)	-541	1.85	284 (La)	-498	1.75
V200	328 (La)	709	2.16	318 (La)	653	2.07

Table 12. Design moment and shear comparisons - Multi-span bridge

Final Girder Designs

The primary objectives of this study was to create a number of pairs of single span composite steel girder bridge designs and at least one pair of multi-span girder designs to serve as test cases for comparing the AASHTO ASD and LRFD highway bridge design codes. The single span bridge designs were created using each of the two AASHTO codes for bridges containing 4, 5, and 6 girders and span lengths of 22.86 m (75 ft) and 45.72 m (150 ft). Rolled shapes were used for the 22.86 m span, and plate girders were used for the 45.72 m span. The multi-span bridge has similar roadway dimensions, and consists of two 30 m side spans and a 50 m center span. The bridges were designed to be the most efficient cross section allowed by each code, within the accuracy allowed by the use of hand design methods, in order to allow the comparison of the ASD and LRFD codes as they are applied to rolled shapes and plate girders. Since the "most efficient" designs from a strict mathematical viewpoint may not use realistic dimensions for fabrication, a second set of tables is also provided, by scaling up the dimensions from the "most efficient" to the "buildable" girders. In determining the buildable girders, plate thicknesses that are readily available from fabricators were selected, and all plates were varied by minimum increments of 25 mm. In selecting the "buildable" designs, the exterior plate girders were resized to be at least as large as the interior girders, if the design calculations permitted smaller girders.

Single Span ASD Girder Designs

Tables 13 and 14 contain the dimensions for the final girder designs of the single span bridges as calculated using the AASHTO ASD code. All values are presented in metric units (mm, mm^2, and kg).

	Rolled Shape	Web	Flanges	Cover Plate	Area Steel
22.86 m - 6 Girders	W920x201	903 x 15.2	304 x 20.1	355 x 18	31990
22.86 m - 5 Girders	W1000x249	980 x 16.5	300 x 26	350 x 18	38000
22.86 m - 4 Girders	W1000x296	982 x 16.5	400 x 27.1	450 x 23	48050

Table 13: 22.86 m (75 ft) – ASD rolled section designs - Single span bridges

	Web	Top Flange	Bottom Flange	Area Steel
45.72 m - 6 Girders	1948 x 14	395 x 22	590 x 30	53662
45.72 m - 5 Girders	2147 x 15	495 x 23	685 x 30	64140
45.72 m - 4 Girders	2238 x 16	600 x 26	795 x 36	80028

(a) "Most efficient" girder sections

	Web	Top Flange	Bottom Flange	Area Steel
45.72 m - 6 Girders	1950 x 14	400 x 22	600 x 30	54,100
45.72 m - 5 Girders	2150 x 15	500 x 23	800 x 30	67,750
45.72 m - 4 Girders	2250 x 16	600 x 28	800 x 38	83,200

(b) "Buildable" girder section

Table 14: 45.72 m (150 ft) – ASD plate girder designs - Single span bridges

For both the rolled section designs presented in Table 13 and the plate girder designs summarized in Table 14, the allowable stress bending provision, Group I, controlled the design of each girder. This provision relates to the normal bending load case. In addition to this criterion, the web bend buckling provision played an important role in sizing the plate girders. In some instances, the Group 1A bending provision would be satisfied, but due to a relatively high bending stress and a low web depth to thickness ratio, the bend buckling criterion was not satisfied, and the thickness of the web and/or tension flange had to be adjusted.

In each of the ASD girder designs, both rolled shapes and plate girders, the same girder was used for all girders in each bridge, despite the fact that the loads the exterior girders carry are less than those on the interior. This is necessary because the ASD code does not allow the exterior girders to have less load carrying capacity than the interior girders under any circumstances to allow for expansion of the roadway.

Single Span LRFD Girder Designs

Tables 15 and 16 contain the dimensions for the final girder designs of the single span bridges, as calculated using the AASHTO LRFD code. As in the ASD girder design tables, all values are presented in metric units (mm, mm^2, and kg).

	Interior Exterior	Rolled Shape	Web	Flanges	Cover Plate	Area Steel
22.86 m - 6 Girders	Int	W760x134	750 x 11.9	264 x 15.5	341 x 22	24502
	Ext	W760x134	750 x 11.9	264 x 15.5	347 x 31	27757
22.86 m - 5 Girders	Int	W920x201	903 x 15.2	304 x 20.1	345 x 12	29848
	Ext	W920x201	903 x 15.2	304 x 20.1	345 x 11	29494
22.86 m - 4 Girders	Int	W1000x222	970 x 16	300 x 21.1	350 x 19	34950
	Ext	W1000x223	970 x 16	300 x 21.1	350 x 13	32850

Table 15: 22.86 m (75 ft) – LRFD rolled section designs - Single span bridges

	Interior Exterior	Web	Top Flange	Bottom Flange	Area Steel
45.72 m - 6 Girders	Int	1800 x 13	340 x 18	540 x 24	42480
	Ext	1800 x 13	365 x 19	565 x 26	45025
45.72 m - 5 Girders	Int	1900 x 14	350 x 18	610 x 26	48760
	Ext	1900 x 14	370 x 18	600 x 27	49460
45.72 m - 4 Girders	Int	2000 x 15	395 x 21	690 x 30	58995
	Ext	2000 x 15	365 x 19	665 x 28	55555

(a) "Most efficient" girder design

	Interior Exterior	Web	Top Flange	Bottom Flange	Area Steel
45.72 m - 6 Girders	Int	1800 x 13	350 x 18	550 x 25	43,450
	Ext	1800 x 13	375 x 19	575 x 28	46,625
45.72 m - 5 Girders	Int	1900 x 14	350 x 18	625 x 28	50,400
	Ext	1900 x 14	375 x 18	625 x 28	50,850
45.72 m - 4 Girders	Int	2000 x 15	400 x 22	700 x 30	59,800
	Ext	2000 x 15	400 x 22	700 x 30	59,800

(b) "Buildable" girder design

Table 16: 45.72 m (150ft) – LRFD plate girder designs

The serviceability II limit state criterion controlled the designs for all but one set of girders for the LRFD rolled shapes and plate girders summarized in Tables 15 and 16 respectively. This service limit state controls local yielding of steel structures due to vehicular live load, which may cause undesirable permanent deflection. However, the interior and exterior girder designs of the 22.86 m span with 6 girders were controlled by the ductility provision contained in the Strength I limit state check for bending. This ductility criterion is the requirement that must be satisfied in order to use a nominal flexural resistance greater than the yield stress. The allowance of a capacity higher than the yield moment is an important revision in the AASHTO code as it allows the engineer to make significant material savings, despite having higher design loads than those in the ASD code. This conclusion depends upon the load and resistance factors as well as the higher allowable moments. If the load factors were set sufficiently high, and the resistance factors sufficiently low, a heavier, not lighter section would result. The load and resistance factors were set to insure a dependable, consistent probability of failure. Therefore, increasing the load factors, or decreasing the resistance factors would, in effect, change the target failure probability.

One of AASHTO's revisions in the LRFD code permits exterior girders to be smaller than the interior girders in cases where expansion of the roadway is not possible. Although in most cases it would not be possible to rule out future bridge lane expansion, this assumption was made in the design of the bridge models so that the material savings associated with this code change could be evaluated. Of the six LRFD bridge design cases considered in the current study, half of cases included exterior girders that required more carrying capacity than the interior girders. For the other six cases, a certain amount of material saving was possible. Upon examining the amount of steel used, it was found that a savings of only up to 3% of the bridge's total steel used could be made with smaller exterior girders, a seemingly negligible amount. Nevertheless, these smaller exterior girders were modeled in the finite element analyses

conducted in this study. If this assumption was dropped, and the exterior girders were sized the same as the interior girders, a slight increase in the total amount of steel in the LRFD bridge designs would be seen.

Multi-Span Girder Designs

The ASD and LRFD designs for negative and positive bending sections of the three span, 6 girder bridge are summarized in Table 17. The LRFD designs for this bridge were controlled by the Strength I limit state. The absence of full lateral support in this case made it uneconomical to develop the plastic moment capacity in the negative bending region, and absent this, it was considered undesirable to use the plastic moment capacity in the positive moment region. Therefore, since maximum bending stresses were limited to be below F_y under the strength I limit state, it was unlikely that the serviceability II limit state, which has smaller load factors, would control.

Negative Bending Section Design Comparison					
	ASD Design		LRFD Design		
Item	Dimensions	Area	Dimensions	Area	Area Ratios
Flanges	27 x 480	12,960	26 x 500	13,000	1.00
Web	13 x 1800	23,400	12 x 1800	21,600	0.92
Total Area		49,320		47,600	0.97
Positive Bending Section Design Comparison					
	ASD Design		LRFD Design		
Item	Dimensions	Area	Dimensions	Area	Area Ratios
Compression Flange	16 x 280	4,480	16 x 350	5,600	1.25
Tension Flange	20 x 440	8,800	20 x 450	9,000	1.02
Web	13 x 1800	23,400	10 x 1800	18,000	0.77
Total Area		36,680		32,600	0.89

Table 17. Multispan Girder Design Summary

Live Load Deflection Analysis

One of the primary goals of the current study is to determine how the changeover from ASD to LRFD bridge design codes will affect the flexibility of the resulting bridges. As discussed in the previous sections, the LRFD code consistently produces girders with smaller cross-sectional areas than those produced by the ASD code. This suggests that the LRFD girders will be more flexible than the ASD girders. To determine how significant this change is, a deflection analysis must be conducted to determine the maximum deflections of each bridge under a specified loading. AASHTO (1998), Section [3.6.1.3.2] stipulates that if the optional deflection limits are invoked, then this loading shall be taken as the larger of the design truck or 25% of the design truck in combination with lane loading. The design truck was found to be more critical for the girders in this study, so it is the loading used in the deflection analysis. The load case involving a quarter of the design truck and the full design lane would only control in much longer spans.

Neither the ASD nor the LRFD code specifies a specific technique for determining the maximum deflection; so two options are explored in this study. An example of each deflection

	22.86 m (v_{max} = 28.6 mm)		45.72 m (v_{max} = 57.2 mm)	
	ASD	**LRFD**	**ASD**	**LRFD**
6 Girder	14.4	21.2	20.4	31.4
5 Girder	12.8	19.3	17.0	29.3
4 Girder	11.2	17.3	14.8	27.0

Table 18: Maximum deflections (mm)calculated by lumped moment of inertia method

analysis is included in Simons (2005). The first deflection analysis involves treating the entire bridge as a simple beam. This is accomplished by combining the short-term composite section properties of each girder to determine an effective moment of inertia for the entire bridge. Using this first deflection analysis yielded the maximum deflections that follow in Table 18.

As predicted, the LRFD bridges are all more flexible than the ASD bridges. None of the maximum deflections calculated by the first method is close to exceeding the optional deflection limit of L / 800. It is also interesting to note the stiffness of each bridge increases as fewer girders are used, despite having a lower area of steel for the entire bridge. This suggests that by having fewer deeper beams instead of more shallow beams, a material savings is possible through the LRFD code, and the bridges will tend to be less flexible.

Rather than viewing the bridges as simple beams, the second deflection analysis treats each girder by applying the live loads with distribution factors. Each ASD and LRFD girder is subjected to the design truck load factored by the corresponding distribution factors. Since the exterior and interior girders would provide different results in many cases, the deflections of a bridge's girders are combined by a weighted average, which assumes that the exterior and interior girders have equal contributions to the bridge's stiffness. The maximum deflections calculated by this second method are included in Table 19.

As in the previous analysis, the LRFD girders are more flexible than the ASD girders. In fact, using the distribution factors to determine the appropriate loading for deflection analysis, the 22.86 m LRFD span with 6 girders no longer satisfies the optional deflection criterion of L / 800. This is the same bridge whose girders were controlled by the ductility requirement rather than the serviceability II limit state.

In referring to Tables 18, and 19, one additional observation is in order. The shorter span bridges had larger deflections as a proportion of length than did the longer span bridges, regardless of whether the ASD or LRFD specifications were used to produce the design, and regardless of the method that was used to compute the deflections. This is not surprising, since

	22.86 m (v_{max} = 28.6 mm)		45.72 m (v_{max} = 57.2 mm)	
	ASD	**LRFD**	**ASD**	**LRFD**
6 Girder	20.5	30.1	28.9	40.0
5 Girder	18.2	25.7	24.3	36.4
4 Girder	16.0	21.8	21.0	32.0

Table 19: Maximum deflections (mm) calculated by distribution factor method

the dead load will tend to be a larger proportion of the total load as the span increases, and it suggests that service load deflection limits are more likely to be exceeded for relatively short bridges.

DISCUSSION

Design Procedure

A preliminary design procedure was presented in the methods section that was used in the current project to facilitate obtaining first guesses of the section properties. Although the equations presented for use in the preliminary design procedure appear complicated at first, they are easily implemented on a computer worksheet. Subsequent to initial programming, the coefficients used in the preliminary design calculations are quickly obtained by simply entering approximate ratios. The resulting preliminary designs appear to be relatively insensitive to at least some of the initial guesses. These preliminary design strategies were used extensively in developing the bridge designs in the current study. Although complete comparisons have not been obtained at this time, preliminary comparisons of the designs obtained in the study with a recently obtained software program indicate that the designs reported here are both feasible (i.e. satisfy the design constraints) and efficient. In almost all cases, the first design estimates obtained using one or two iterations of the preliminary designs either satisfied the design conditions closely, or were sufficiently close that only minor section revisions had to be made.

The designs were finalized by comparing with the strength, serviceability, and fatigue limit states, and any changes in section suggested by the limit states were made. Typically, these changes were relatively small, so that each design step could be carried out efficiently, at least for the single span bridges.

The process becomes significantly more complicated when a multispan bridge is being designed, since the girder line design/analysis cycle needs to be carried out iteratively. Different girder sections are used in positive and negative bending regions. Moreover, the slab is not effective in negative bending at the strength limit states, so several cycles of statically indeterminate analysis may be required to obtain a convergent design. During these cycles, the moments will tend to shift from negative bending to positive bending regions. This procedure is extremely tedious to carry out by hand, and suggests that structural design software is essential for efficient design.

Live Load Models and Load Application Procedures

Dynamic Load Allowances and Impact Factors

As indicated in Tables 1 and 2, the AASHTO LRFD dynamic load allowances are somewhat larger than the AASHTO ASD impact factors. This difference appears to increase as the span length increases, since the ASD factors decrease as span length increases, while the LRFD factors are independent of span length. The AASHTO LRFD factors appear to be comparable to those specified by the current Ontario Highway Bridge Design Code. This finding

is perhaps overly simplified, however, since not only the factor, but also the load to which the factor is applied must be considered. The ASD impact factor is applied to the total applicable live load moment and shear, while the LRFD factor is applied only to the truck loading model, and not to the lane load model that is subsequently added in. In the current set of design studies, the LRFD truck load moments and shears were typically between 50% and 65% of the total live load, before impact factors or dynamic load allowances are applied. For shorter spans the truck load model would comprise a larger portion of the total, while for longer spans that proportion would tend to decrease. Therefore, the actual dynamic load allowance when applied to the total live load is actually significantly smaller than the nominal value of 0.33. Since the percentage of the live load to which the dynamic load allowance is applied will tend to decrease with span, the *effective* dynamic load allowance will, in fact, decrease as the span length increases, similar to the ASD impact factors.

Distribution Factors

The distribution factors computed for the six pairs of single span bridges are given in Tables 3 and 4, and the corresponding factors for the pair of three span bridges are given in Table 5 and 6. To facilitate direct comparison, the ratios of the LRFD factors to the ASD factors for the six simple span bridges are summarized in Tables 7 and 8 above. The corresponding ratios for the pair of three span bridges are given in the last column of Tables 5 and 6.

Upon examining the ratios in Tables 5 and 7, it appears that the LRFD moment distribution factors for the interior girders are consistently less than the ASD factors and decrease as the span length increases. Also, the disparity between the sets of factors increases as fewer girders are used in the design. However, the LRFD distribution factors for the exterior girders in the current study are consistently larger than those of the ASD code. From the shear ratios shown in Table 6 and 8, the LRFD distribution factors are generally greater than the ASD factors for both interior and exterior girders, but tend to decrease relative to the ASD factors as the number of girders decreases. Further studies including even longer spans may provide additional insight as to these observed trends.

The analysis can be taken one step further by introducing the assumption that the effective widths of bridge supported by the exterior girders are the same as that supported by the interior girders. By making this assumption, a weighted average of these ratios can be calculated to determine the net effect of adopting LRFD distribution factors. The assumption is a reasonable approximation, since the effective widths of bridge supported by the exterior girders are not drastically different than those of the interior girders. This analysis resulted in the weighted average ratios for the full bridges presented in Table 20 for the simple span bridges. This averaging process was not attempted for the multi-span bridge.

	Moment		Shear	
	22.86 m	**45.72 m**	**22.86 m**	**45.72 m**
6 Girders	0.975	0.907	1.117	1.135
5 Girders	0.943	0.884	1.075	1.075
4 Girders	0.902	0.853	1.007	1.007

Table 20. Ratios of LRFD to ASD distribution factors estimated for full bridges - Single span bridges

These values indicate that the LRFD code produces moment distribution factors that have a net effect of about 85 to nearly 100% of the effect of ASD moment distribution factors. The LRFD distribution factors for shear have a net effect of about 100 to 112% of the effect of ASD shear distribution factors. To summarize the distribution factor comparison, on average the LRFD produces lower distribution factors for moment, and produces higher distribution factors for shear than the ASD code. The increases of the shear distribution factors will not likely affect the designs significantly, since shear rarely controls gross section dimensions. Since the bending limit state often controls such designs, the decreases of the moment distribution factors contributes towards decreasing LRFD girder sizes.

Design Live Load Comparison

The live load revision introduced in the first edition of the AASHTO LRFD specification, and continued in the second edition was intended to increase the design live load moments and shears to levels that are considered to be consistent with the results of simulations and measurements on actual bridges. From the above discussion, it is seen that the overall effect of the change in dynamic load allowance is likely to be modest, while the distribution factors may either decrease, or increase the percentage of the moment or shear contributed to the individual girders. In order to evaluate the overall effect, the girder line moments and shears, the distribution factors, and the dynamic load allowances (or impact factors in ASD terminology) were combined to produce design moments and shears. Only once all of the factors have been implemented is it meaningful to compare the resultants, as these are the quantities that are the final input (except for load factors) on the load side of the design equations. The resulting design moments and shears on the six pairs of single span bridges are summarized in Tables 9 and 10 respectively, while the moments and shear for the two pairs of multi-span bridges are summarized in Table 12. The clear result of the analysis is that the AASHTO LRFD design moments and shears are significantly larger than the corresponding quantities used in the ASD design specification. The ratios in Table 11 reflect two trends for single span bridges. As the number of girders decreases, LRFD/ASD design ratios tend to decrease, while as the span length increases, the LRFD/ASD ratios tend to increase. However, in all cases the ratios are greater than 1. The multi-span bridge LRFD/ASD ratios only reflect the results from one girder spacing and one set of spans, so any larger trends cannot be predicted for these ratios. It does appear that the observed trends mirror the trends in the distribution factors, so it is anticipated that similar trends would be observed for multi-span bridges if a number of such structures were designed.

The LRFD/ASD ratios indicate that the LRFD code produces live load moments that range from 8 to 106% larger than the ASD moments, and live load shears that range from 24 to 116% higher than ASD shears. From these results, it appears that the new vehicular live load models had a larger influence on the design loads than the overall decrease in distribution factors, and the rather modest effective changes in the dynamic load allowances.

Comparison of ASD and LRFD Girder Designs

The revisions introduced by the AASHTO LRFD specification were sufficiently sweeping that any systematic changes to be expected in the resulting designs is difficult to evaluate without carrying out a series of comparison designs. Some of the most telling results

can be found simply by comparing the total steel used for each bridge design case. These areas of steel (mm^2 / unit length) are presented in Table 21 for each of the single span bridges, and are illustrated in Figures 3 and 4.

	22.86 m - ASD	22.86 m - LRFD	45.86 m - ASD	45.86 m - LRFD
6 Girders	191940	153522	321972	259970
5 Girders	190000	148532	320700	245200
4 Girders	192200	135600	320112	229100

Table 21: Total area of steel for each bridge design case - Single span bridges

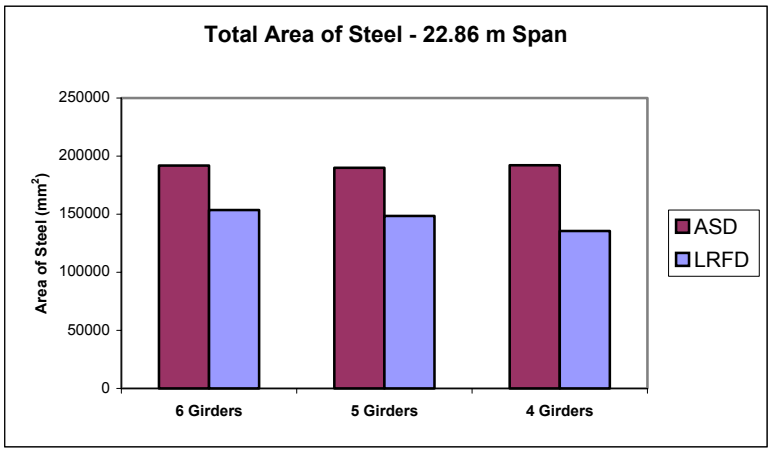

Figure 3: Total area of steel in single span rolled section bridges

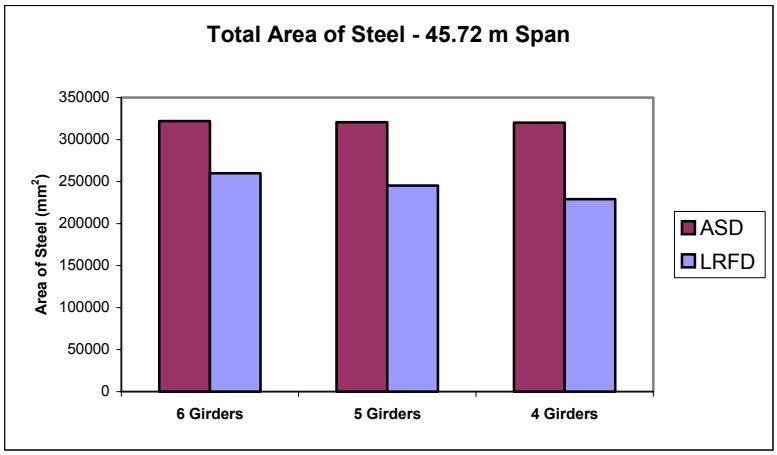

Figure 4: Total area of steel in single span plate girder bridges

For each of the single span composite girder bridges considered in this study, using the AASHTO LRFD code instead of the ASD code significantly reduced the total area of steel used in the longitudinal girders, despite being required to carry much higher design loads. As shown in Table 22, a 20 – 30% material savings is observed when using the LRFD code.

It is also interesting to note the effect of the number of girders per span. For the ASD bridges, changing the number of girder had no discernable effect upon the total area of steel. For the LRFD bridges however, a noticeable additional material savings is made as fewer girders are

	22.86 m	45.72 m
6 Girders	20.0%	19.3%
5 Girders	21.8%	23.5%
4 Girders	29.4%	28.4%

Table 22: Percent decrease in area of steel by using LRFD code - single span bridges

used. This savings is potentially a significant advantage of the AASHTO LRFD code. Using the LRFD code provides the engineer with more options for cutting material costs. It can be inferred from these material savings results that the LRFD bridges will, in all likelihood, be more flexible than the ASD bridges; however, this consideration will be analyzed explicitly later in this report.

It is likely that the material savings discussed above is primarily due to a relaxation of the bending stress provisions in the LRFD code. The normal bending case controlled each of the ASD bridge designs. In the LRFD code, the strength I limit state corresponds with the normal bending case. Regarding this limit state, a provision is included that allows the nominal moment capacity to exceed the yield moment under the condition that a ductility requirement is satisfied. This allowance of nominal capacity in the plastic region is not permitted by the ASD code. Therefore it is reasonable that the strength I criterion in the LRFD may not control except in cases of shallow rolled sections. Instead, the design of the majority of the single span bridges in this study were governed by the LRFD serviceability II limit state for permanent deflection. It appears that these code revisions allow the LRFD bridges to use less steel than the ASD bridges, despite the fact that they are required to carry higher design loads.

This conclusion does not fully extend to multi-span bridges, for which additional complications associated with the un-braced negative bending regions may have a significant influence upon the design. The LRFD design of the three-span six girder bridge considered in this project tended to be controlled by the strength I limit state, for both negative and positive bending. This is logical, since the girders were designed as non-compact in the negative bending region, based primarily upon the existence of a laterally un-braced length in excess of L_{pd}, as defined above. As a result the bending stresses under factored loadings were limited by F_y. Actually the stresses were limited to somewhat less than F_y, since the load shedding factor R_b was slightly smaller than 1, indicating web bend buckling at the strength limit state. Therefore, the serviceability II limit state, which limits stresses to $0.95F_y$ with considerably smaller load factors, is less likely to control in this case. In the positive bending region, the rational decision to not allow the use of plastic section capacity, even though the section was locally compact, in view of the much larger curvatures that would be needed to develop the plastic moment, effectively limited the design stresses to F_y as well, and this meant that the strength I limit state tended to provide a more critical criterion than the serviceability II limit state in this case as well.

Generally, the fact that plastic capacity was not used in either negative or positive bending regions in the three-span bridge reduced the material savings achieved using LRFD. LRFD led to a reduction in girder cross section of only about 3% in the negative bending region, and 11% in the positive bending region. All of the material savings was a direct result of the

thinner webs permitted by LRFD. It should be noted at this point that additional studies of multi-span bridge designs should be undertaken to further verify these conclusions.

Deflection Analysis

Two different methods of calculation were used to determine deflections in the current study. Even though the AASHTO codes do not stipulate what deflection calculation method should be used, insight can be gained from examining the results of each of the two methods that were used. Both demonstrate that the LRFD code produces more flexible girders than the ASD code. This is shown result is summarized in Table 23.

	Method One		Method Two	
	22.86 m	**45.72 m**	**22.86 m**	**45.72 m**
6 Girders	47%	54%	47%	38%
5 Girders	51%	72%	41%	50%
4 Girders	54%	83%	37%	52%

Table 23. Percent increase in maximum deflection resulting from using LRFD code

The bridges designed using the LRFD code in the current study are between 37 and 83% more flexible than the ASD bridges. This trend is more pronounced in the longer spans. In most cases, the LRFD bridges still pass the optional deflection criteria, but the shortest and shallowest girder bridge did not meet the limit. Since this was the only LRFD bridge to be controlled by the ductility provision instead of the serviceability II criterion, these results suggest that bridges controlled by ductility may have more problems with excessive flexibility. This conclusion should be regarded as purely preliminary, and should be subject to further design tests. It is not possible to determine the suitability of this optional deflection limit without studying actual bridges with flexibility issues. Additionally, it should be noted that each of the bridge designs passed the optional slenderness ratio limit (depth / span > 1/30), though the most flexible bridge was the closest to the limit at a depth to span ratio of 1 / 29.6. Therefore, it does seem that both optional limits convey some indication of a bridge's flexibility.

Deflection calculations were not completed on the multi-span bridge. However, preliminary calculations indicate that the relatively similar areas of material (except for the web steel) in the LRFD and ASD designs led to similar flexibility in the both LRFD and ASD designs. This is also reflected in natural frequency calculations, reported in Baber and Simons (2005) that indicate almost identical first bending frequencies for multi-span girder designs.

CONCLUSIONS

The following conclusions relevant to the design process and the results of the design process were reached.

Design Process

Several approximate design tools were developed in the process of comparing the AASHTO ASD and LRFD bridge design specifications. First estimate methods were developed for both the ASD and LRFD design, and both of these methods yielded sections that converged quickly to efficient section designs. These methods provided a useful starting point in the designs.

The calculations involved in LRFD design are lengthy, and considerably more complicated than those needed for ASD design. For example, the distribution factors, needed at the beginning of the design, are a function of the bridge girder/slab stiffness ratio, which is not known until after the design. An approximation that ignores this term in the initial distribution factor estimates provides a reasonable first estimate of the distribution factors, but the final values of the distribution factors require that the calculated girder properties be used to revise the loadings, even for simple span girders.

Design Moments and Shears

Driven by the more restrictive live load models, the final LRFD design live load moments and shears proved to be considerably higher than the ASD design live loads. These design loads were affected by the following trends:

- The LRFD code's superposition of the design lane load upon the design truck and design tandem provides larger loads than the three loadings separately.

- The LRFD constant dynamic load allowances are more conservative than the impact factors provided by the ASD code. The final effect of this increase is not large however, since the increased factor is applied only to the truck load, and not to the superimposed lane load.

- The revised LRFD distribution factor method is tends to produce smaller moment distribution factors and somewhat larger shear distribution factors than the method provided by the ASD code.

These trends in load approximation and application caused an overall increase in design live loads. LRFD live load design moments increased by 8 – 99% relative to ASD values, and design shears increased by 24 – 90%. These design live load increases were most pronounced in the longest spans, where the superimposed lane load moment had the most significant effect. The increases were also larger in the bridges with the most girders.

Girder Designs

The girders designed using the LRFD specifications typically required less steel than the girders designed using the ASD code. For the six simple span design cases considered in this

study, a material savings (area of steel per unit length) of 20 – 30% is observed over the entire bridge when using the LRFD specification. In addition, the bridges designed using the LRFD code became more efficient as fewer girders were used; such savings were not systematically obtained using the ASD code in the current study. This material savings appears to be attributed the use of bending resistances in excess of the yield moment in LRFD design. When design stresses were limited to F_y, as was the case in the three span girder designs, the material savings decreased between 3% and 10%, which was attributed to the thinner webs permitted by the LRFD specification.

By permitting the nominal moment capacity to exceed the yield moment under the condition that a ductility requirement is satisfied, the LRFD code does not generally produce girders that are governed by the basic bending load case. Instead, the majority of the LRFD bridge designs are controlled by the Serviceability II limit state, which corresponds to the Group IA load combination of the ASD code.

The LRFD specifications produced more flexible bridges than the ASD specifications, consistent with the reduction in girder cross-sectional areas. The simple span LRFD bridges were 37 – 83% more flexible than the ASD girders as measured by live load deflection; this flexibility was more pronounced in bridges containing more girders. Thus when using the LRFD specifications, using fewer girders in design appears to save material and increase stiffness when the entire bridge is considered. Each bridge satisfied the depth to span ratio requirement of 1/30. Only one simple span bridge violated the optional deflection criterion (L/800), the 22.86 m (75 ft) span with 6 girders designed using the LRFD code. This is also the only simple span LRFD bridge design that was controlled by the ductility requirement in the Strength I limit state, rather than the Serviceability II limit state. The multi-span bridges designed by LRFD and ASD specifications appeared to have similar stiffness. The increased flexibility appears to be a direct consequence of permitting moments in excess of M_y at the strength I limit state. Where non-compact section conditions limited the maximum bending stress to F_y, the LRFD code produced girders of comparable stiffness to the ASD code.

RECOMMENDATIONS

1. *Based upon our experience in this project, VDOT's Structure & Bridge Division should continue to support training in AASHTO's LRFD code.* Since this study was completed, VDOT's Structure & Bridge Division has moved forward in the implementation of the LRFD code by:

    - evaluating and selecting a series of design software packages to ensure consistent, efficient, and code compliant bridge designs

    - training VDOT's structural engineers in the LRFD code and the accompanying software packages.

2. *There does not appear to be sufficient evidence available at this time to recommend increasing the stringency of the deflection requirement, but the L/800 deflection limit should be retained until the specific causes of premature deck deterioration have been more fully identified.* A primary objective of this study was to investigate whether bridges designed using the LRFD code were more or less likely to exceed deflection limits than bridges designed using the AASHTO ASD code in view of the increased design live loads. The increased flexibility observed in the single-span bridges designed using the LRFD code and the comparable flexibility observed in the multi-span design comparison suggest that bridges designed using the LRFD code will tend to be at least as flexible as, and often more flexible than, bridges designed using the ASD code even though they are designed for larger live loads. Although it has not been demonstrated conclusively that more flexible bridges tend to deteriorate more rapidly, it does not appear advisable to ignore the deflection limits at this time. In view of the design results obtained in this study, it does not appear that the cost of retaining these limits will be large, and the extra effort required during the design stage can be reduced by the use of comprehensive bridge design software that includes the deflection limits check in the automated design procedure.

SUGGESTIONS FOR FUTURE STUDIES

Although this study answered many questions regarding the nature of changes to be expected in bridges designed using the LRFD code relative to those designed using the ASD code, additional topics remain unexplored by the current project; for example:

- Following observations that local instead of overall bridge deformation might be a more significant contributor to bridge deck deterioration, a study of potential local deformation limits that might be more applicable to deck deterioration than AASHTO's global deflection limits should be undertaken.

- Further comparison of the LRFD and ASD codes for multi-span bridges with composite girders, girders with longitudinally stiffened webs, and skew bridges will provide additional data points that will reinforce the conclusions reached in this study.

COSTS AND BENEFITS ASSESSMENT

The transition from AASHTO's ASD code to AASHTO's LRFD code may be expected to lead to lighter weight girders in general. In the studies considered here, the girders for bridges designed using the LRFD code were 20% to 30% lighter for single-span bridges and from 3% to 11% lighter for the three-span continuous bridge considered. There may be slight differences in fabrication costs, but most of the percentages in weight savings will roll over into direct savings in initial costs because steel is bought by the pound. However, the cost savings is accompanied by increased flexibility, which may be a contributing factor in premature deck deterioration.

As stated in the Recommendations, the optional deflection limits should be retained in VDOT design practice. Increasing the stringency of the limits is not warranted at this time. Retaining the deflection limits may slightly reduce the materials savings that would be expected for some single-span bridges. The multi-span bridges designed by the LRFD code using the methods described in this study did not appear to be substantially more flexible than those designed using the ASD code, so a significant decrease in material savings would not be expected for these bridges.

ACKNOWLEDGMENTS

The authors thank the Virginia Transportation Research Council for the financial support of this project. Dr. Jose Gomez of VTRC is also acknowledged for his comments and critiques throughout the project.

REFERENCES

Agarwal, A.C., and Wolkowicz, M., (1976), *Interim report on 1975 commercial vehicle survey*, Research and Development Division, Ministry of Transportation, Downsview, Ontario, Canada.

AASHTO, (1992), *Standard Specifications for Highway Bridges*, 15th ed., Washington, DC.

AASHTO, (2002), *Standard Specifications for Highway Bridges*, 17th ed., Washington, DC.

AASHTO, (1998), *AASHTO-LRFD Bridge Design Specifications – Customary US Units*, second edition, Washington, DC.

American Society of Civil Engineers, (1958), Deflection Limitations of Bridges - Progress Report of the Committee on Loads and Forces on Bridges of the Committee on Bridges of the Structural Division, *Journal of the Structural Division*, ASCE, 84, ST3, 1633-1 to 1633-20.

American Institute of Steel Construction, (2001), *Manual of Steel Construction: Load and Resistance Factor Design*. 3rd Edition.

Baber, T.T., and Simons, D.C., (2005), *AASHTO LRFD Impact upon Bridge Stiffness and Strength: II - Modal Analysis and Comparison*, Virginia Transportation Research Council, Charlottesville.

Barefoot, J., (1995), Development of Bridge Models. M.S. Thesis, University of Virginia, Charlottesville.

Barker, R.M., and J.A. Puckett, (1997), *Design of Highway Bridges*. John Wiley & Sons, Inc., New York.

Basler, K., (1961), Strength of Plate Girders in Bending, *Journal of the Structural Division*, ASCE, Vol. 87, ST4, 153-181, August.

Buckland, P.G., (1991), North American and British Long-Span Bridge Loads, *ASCE Journal of Structural Engineering*, 117(10), 2972-2987.

Hwang, E.S., and Nowak, A.S., (1991), Simulation of dynamic load for bridges, *Journal of Structural Engineering*, ASCE, 117, 5, 1413-1434.

Kulicki, J.M., and Mertz, D.R., (1991), A New Live Load Model for Bridge Design, *Proceedings of 8th Annual International Bridge Conference*, Pittsburgh, PA.

Kulicki, J. M., (2005), Past, Present and Future of Load and Resistance Factor Design: AASHTO LRFD Bridge Design Specifications, *Proceedings of 6th International Bridge Engineering Conference*, Boston MA.

Melchers, R.E., (2001), *Structural Reliability Analysis and Prediction*, 2d Edition, John Wiley & Sons, Chichester.

Mueller, J.A., and Yen, B.T., (1968), Girder Web Boundary Stresses and Fatigue, *WRC Bulletin No. 127*, January.

Nowak, A.S., (1993), Calibration of LRFD Bridge Design Code. *National Cooperative Highway Research Program*, Project 12-33.

Nowak, A.S., (1999,) Calibration of LRFD Bridge Design Code. *National Cooperative Highway Research Program*, Report 368.

Nowak, A.S., and Hong, Y-K., (1991), Bridge Live Load Models, *Journal of Structural Engineering*, ASCE, 117, 9, 2757-2767.

Salmon C.G., and Johnson, J.E., (1996), *Steel Structures: Design and Behavior*, Harper Collins, New York.

Simons, D.C., (2005), *AASHTO LRFD Impact upon Bridge Stiffness and Strength*, M.S. Thesis, University of Virginia, Charlottesville.

Taly, N., (1998), *Design of Modern Highway Bridges*. The McGraw-Hill Companies, Inc., New York.

Tilley, M., (2004), Analysis of a Curved Girder Bridge, M.S. Thesis, University of Virginia, Charlottesville.

Wittry, D.M., (1993), An Analytical Study of the Ductility of Steel Concrete Composite Sections, M S. Thesis. University of Texas at Austin.

Wollmann, G. P., (2004a), Steel Girder Design per AASHTO LRFD Specifications (Part 1), *Journal of Bridge Engineering*, Vol. 9, No. 4, July.

Wollmann, G.P., (2004b) ,Steel Girder Design per AASHTO LRFD Specifications (Part 2), *Journal of Bridge Engineering*, Vol. 9, No. 4., July.

Wright, R. N. and Walker, W. H. (1971) Criteria for Deflection of Steel Bridges, *AISI Bulletin*, No. 19, November.

Yen, B.T., and Mueller, J.A., (1966), Fatigue Tests of Large Size Welded Plate Girders, *WRC Bulletin No. 118,* November.

Zokaie, T., (1991), Distribution of Wheel Loads on Highway Bridges. *Research Results Digest*, No. 187. National Cooperative Highway Research Program, Project 12-26.

Zokaie, T., (2000), AASHTO-LRFD Live Load Distribution Specifications. *Journal of Bridge Engineering*, Vol. 5, No. 2, May.

APPENDIX A
MATHCAD POSITIVE SECTION ELASTIC ESTIMATOR

Elastic Section Ratios Estimator: This worksheet, for use in preliminary designs, provides estimates of the section moduli as functions of the product $A_{tf}D$ for use in obtaining design estimates for welded plate girders. The calculations may be used either in ASD or in LRFD, if the strength is limited by the yield stress. For composite sections, LRFD lower bound estimates should start with a simple plastic section modulus calculation, instead. The accuracy of the ratio estimates depends upon the accuracy of the α values input at the very beginning of the worksheet. However, even with relatively bad estimates on the first pass, a couple of iterations yields a useful and fairly efficient section.

Input: Estimate ratios of slab area, web area and compression flange area to tension flange area and provide modular ratio.

$\alpha_{sl} := 37$ $\alpha_{web} := 1.6$ $\alpha_{cf} := 0.5$ $n := 8$

Calculate ratios for Non-composite section

$$C_0 := \frac{0.01 + 0.52\cdot\alpha_{web} + 1.03\cdot\alpha_{cf}}{1 + \alpha_{web} + \alpha_{cf}}$$

$$C_1 := \left[(C_0 - .01)^2 + \frac{\alpha_{web}}{12} + (C_0 - .52)^2\cdot\alpha_{web} + (1.03 - C_0)^2\cdot\alpha_{cf} \right]$$

$$C_{TNC} := \frac{C_1}{1.04 - C_0}$$

$$C_{BNC} := \frac{C_1}{C_0}$$

$C_0 = 0.438$ $C_1 = 0.503$ $C_{TNC} = 0.834$ $C_{BNC} = 1.148$

Calculate ratios for Long-term composite section

$$C_{0LT} := \frac{0.01 + 0.52\cdot\alpha_{web} + 1.03\cdot\alpha_{cf} + 1.11\cdot\frac{\alpha_{sl}}{3\cdot n}}{1 + \alpha_{web} + \alpha_{cf} + \frac{\alpha_{sl}}{3n}}$$

$$C_{1LT} := \left(C_{0LT} - .01\right)^2 + \frac{\alpha_{web}}{12} + \left(C_{0LT} - .52\right)^2 \cdot \alpha_{web} + \left(1.03 - C_{0LT}\right)^2 \cdot \alpha_{cf} + \frac{\alpha_{sl}}{3 \cdot n} \cdot \left(1.11 - C_{0LT}\right)^2$$

$$C_{TLT} := \frac{C_{1LT}}{1.04 - C_{0LT}}$$

$$C_{BLT} := \frac{C_{1LT}}{C_{0LT}}$$

$C_{0LT} = 0.66102$ $C_{1LT} = 0.968$ $C_{TLT} = 2.554$ $C_{BLT} = 1.464$

Calculate ratios for short-term composite section

$$C_{0ST} := \frac{0.01 + 0.52 \cdot \alpha_{web} + 1.03 \cdot \alpha_{cf} + 1.11 \cdot \frac{\alpha_{sl}}{n}}{1 + \alpha_{web} + \alpha_{cf} + \frac{\alpha_{sl}}{n}}$$

$$C_{1ST} := \left(C_{0ST} - .01\right)^2 + \frac{\alpha_{web}}{12} + \left(C_{0ST} - .52\right)^2 \cdot \alpha_{web} + \left(1.03 - C_{0ST}\right)^2 \cdot \alpha_{cf} + \frac{\alpha_{sl}}{n} \cdot \left(1.11 - C_{0ST}\right)^2$$

$$C_{TST} := \frac{C_{1ST}}{1.04 - C_{0ST}}$$

$$C_{BST} := \frac{C_{1ST}}{C_{0ST}}$$

$C_{0ST} = 0.84023$ $C_{1ST} = 1.341$ $C_{TST} = 6.714$ $C_{BST} = 1.596$

APPENDIX B
MATHCAD NEGATIVE SECTION ESTIMATOR

Negative Bending Section Estimation Worksheet (NMWS.mcd):

---

1. Basic Ratio Input

Area Ratios: $\alpha_w := 2$ $\alpha_R := 0.15$

Height Ratios: $\gamma_{cf} := 0.02$ $\beta_R := 0.05$

Yield Strength Ratio: $\rho_y := 1.2$

---

2. Non-composite Section Ratios

$C_{0NC} := 0.5 + \gamma_{cf}$ $C_{0NC} = 0.52$

$C_{1NC} := \frac{\alpha_w}{12} + \frac{\left(1 + \gamma_{cf}\right)^2}{2}$ $C_{1NC} = 0.687$

$C_{TNC} := \frac{C_{1NC}}{C_{0NC}}$ $C_{TNC} = 1.321$

$C_{BNC} := C_{TNC}$ $C_{BNC} = 1.321$

3. Composite Section Ratios

$DC_{0C} := \frac{\left(0.5 + \gamma_{cf} + \beta_R\right) \cdot \alpha_R}{2 + \alpha_R + \alpha_w}$ $DC_{0C} = 0.021$

$C_{1C} := C_{1NC} + \left(2 + \alpha_w\right) \cdot DC_{0C}^{\ 2} + \alpha_R \cdot \left(C_{0NC} + \beta_R - DC_{0C}\right)^2$ $C_{1C} = 0.734$

$C_{TC} := \frac{C_{1C}}{C_{0NC} - DC_{0C}}$ $C_{TC} = 1.469$

$$C_{BC} := \frac{C_{1C}}{C_{0NC} + DC_{0C}} \qquad C_{BC} = 1.357$$

4. Plastic Section Ratios

$$C_p := \frac{\alpha_w + \rho_y \cdot \alpha_R}{2\alpha_w} \qquad C_p = 0.545$$

$$C_Z := \left(C_p^{\,2} - C_p + 0.5\right) \cdot \alpha_w + 1 + \gamma_{cf} + \left(1 - C_p + \gamma_{cf} + \beta_R\right) \cdot \rho_y \cdot \alpha_R \qquad C_Z = 1.619$$

Check plastic to elastic section modulus ratios for composite section

$$\frac{C_Z}{C_{TC}} = 1.101 \qquad \frac{C_Z}{C_{BC}} = 1.192$$

These look to be about right, for a section that is dominated by the plate girder area.

APPENDIX C
MATHCAD SECTION DESIGN WORKSHEET

An example of the worksheets used to perform many of the design calculations is contained in this Appendix. The file contains the calculations for the LRFD design of the six girder, exterior plate girder for the 45 m (150 ft) span. Additional worksheets for ASD and LRFD design have been included in the appendices of Simons (2005).

LRFD - 6 Girder - 150 ft Span - Exterior Beam - Plate Girders

Section Calculation Worksheet:

1. Input Section

Slab and Rebar Dimensions:

$t_s := 190$ $b_s := 244($ $t_h := 25$ $n := 8$

$d_p := 53$ $d := t_s - 33$

$A_{rt} := 100($ $A_{rb} := 140($

Girder Dimensions:

$b_t := 39($ $t_t := 18$ $b_b := 565$ $t_b := 26$

$t_w := 13$ $D := 180($ $h := t_t + t_b + D$ $h = 1.844 \times 10^3$

---

2. Calculate areas of interest, and centroidal locations relative to top of flange

$A_{sl} := t_s \cdot b_s$ $A_{sl} = 4.636 \times 10^5$ $d_{sl} := t_h + \frac{t_s}{2}$ $d_{sl} = 120$

$A_t := b_t \cdot t_t$ $A_t = 7.02 \times 10^3$ $d_t := 0.5 \cdot t_t$ $d_t = 9$

$A_b := b_b \cdot t_b$ $A_b = 1.469 \times 10^4$ $d_b := t_t + D + 0.5 \cdot t_b$ $d_b = 1831$

$A_w := t_w \cdot D$ $A_w = 2.34 \times 10^4$ $d_w := t_t + 0.5 \cdot D$ $d_w = 918$

3. Calculate properties of non-composite section

$A_{beam} := A_t + A_b + A_w$ $A_{beam} = 4.511 \times 10^4$

$M_{1y} := A_t \cdot d_t + A_w \cdot d_w + A_b \cdot d_b$ $M_{1y} = 4.8442 \times 10^7$

$$y_{Tnc} := \frac{M_{1y}}{A_{beam}} \qquad y_{Tnc} = 1073.9$$

$$y_{Bnc} := D + t_t + t_b - y_{Tnc} \qquad y_{Bnc} = 770.1$$

$$I_{nc} := A_t \cdot (y_{Tnc} - d_t)^2 + A_w \cdot (y_{Tnc} - d_w)^2 + A_b \cdot (y_{Tnc} - d_b)^2 + \frac{1}{12} \cdot \left(t_w \cdot D^3 + b_t \cdot t_t^{\,3} + b_b \cdot t_b^{\,3} \right)$$

$$I_{nc} = 2.327 \times 10^{10}$$

$$S_{Tnc} := \frac{I_{nc}}{y_{Tnc}} \qquad S_{Tnc} = 2.167 \times 10^{7}$$

$$S_{Bnc} := \frac{I_{nc}}{y_{Bnc}} \qquad S_{Bnc} = 3.021 \times 10^{7}$$

4. Calculate properties of short-term composite section

$$A_{slst} := \frac{A_{sl}}{n} \qquad A_{stc} := A_{slst} + A_{beam} \qquad A_{slst} = 5.795 \times 10^{4}$$

$$M_{1yst} := A_{beam} \cdot y_{Tnc} - A_{slst} \cdot \left(\frac{t_s}{2} + t_h \right) \qquad A_{beam} = 4.511 \times 10^{4}$$

$$y_{Tst} := \frac{M_{1yst}}{A_{stc}} \qquad y_{Tst} = 402.559$$

$$y_{Bst} := h - y_{Tst} \qquad y_{Bst} = 1.4414 \times 10^{3}$$

$$I_{st} := A_{slst} \cdot \left[\frac{t_s^{\,2}}{12} + \left(\frac{t_s}{2} + t_h + y_{Tst} \right)^2 \right] + A_{beam} \cdot (y_{Tst} - y_{Tnc})^2 + I_{nc} \qquad I_{st} = 5.96 \times 10^{10}$$

$$S_{Tst} := \frac{I_{st}}{y_{Tst}} \qquad S_{Tst} = 1.48 \times 10^{8}$$

$$S_{Bst} := \frac{I_{st}}{y_{Bst}} \qquad S_{Bst} = 4.134 \times 10^{7}$$

5. Calculate properties of long-term composite section

$$A_{sllt} := \frac{A_{sl}}{3 \cdot n} \qquad A_{ltc} := A_{sllt} + A_{beam} \qquad A_{sllt} = 1.932 \times 10^{4}$$

$$M_{1ylt} := A_{beam} \cdot y_{Tnc} - A_{sllt} \cdot \left(\frac{t_s}{2} + t_h \right) \qquad A_{ltc} = 6.443 \times 10^{4}$$

$$y_{Tlt} := \frac{M_{1ylt}}{A_{ltc}} \qquad y_{Tlt} = 715.911$$

$$y_{Blt} := h - y_{Tlt}$$

$$y_{Blt} = 1.128 \times 10^{3}$$

$$I_{lt} := A_{sllt} \cdot \left[\frac{t_s^{2}}{12} + \left(\frac{t_s}{2} + t_h + y_{Tlt} \right)^{2} \right] + A_{beam} \cdot \left(y_{Tlt} - y_{Tnc} \right)^{2} + I_{nc} \qquad I_{lt} = 4.26042 \times 10^{10}$$

$$S_{Tlt} := \frac{I_{lt}}{y_{Tlt}} \qquad S_{Tlt} = 5.951 \times 10^{7}$$

$$S_{Blt} := \frac{I_{lt}}{y_{Blt}} \qquad S_{Blt} = 3.777 \times 10^{7}$$

6. Calculate basic ratios of interest

Web Dimensions (ratios during construction) $D_c := y_{Tnc} - t_t$

$$\frac{2 \cdot D_c}{t_w} \rightarrow 162.439813788516958 \quad \text{less than} \quad 6.77 \cdot \sqrt{\frac{200}{.345}} = 163.002$$

Compression Flange Dimensions

$b_t = 390$ greater than $.3 \cdot D_c = 316.758$

Tension Flange Dimensions

$$\frac{b_b}{2 \cdot t_b} = 10.865 \quad \text{less than} \quad 12$$

Check Iyc/Iy ratio

$$I_{ratio} := \frac{t_t \cdot b_t^{\,3}}{t_t \cdot b_t^{\,3} + t_b \cdot b_b^{\,3}} \qquad I_{ratio} = 0.185 \qquad 0.1 < I_{ratio} < 0.9$$

7. Serviceability II criteria Bending stresses must be less than .328 GPa.

$M_{D1} := 3948$ $M_{D2} := 792$ $M_{D3} := 405$ $M_{LLIM} := 5236$ $M_{FatLLIM} := 1650$

$$\sigma_{T1} := \frac{M_{D1} \cdot 10^6}{S_{Tnc}} \qquad \sigma_{T1} = 182.201$$

$$\sigma_{T2} := \frac{M_{D2} \cdot 10^6}{S_{Tlt}} \qquad \sigma_{T2} = 13.309$$

$$\sigma_{T3} := \frac{M_{D3} \cdot 10^6}{S_{Tlt}} \qquad \sigma_{T3} = 6.806$$

$$\sigma_{T4} := \frac{1.3 \cdot M_{LLIM} \cdot 10^6}{S_{Tst}} \qquad \sigma_{T4} = 45.979$$

$$\sigma_{Ttot} := \sigma_{T1} + \sigma_{T2} + \sigma_{T3} + \sigma_{T4} \qquad \sigma_{Ttot} = 248.293$$

$$\sigma_{B1} := \frac{M_{D1} \cdot 10^6}{S_{Bnc}} \qquad \sigma_{B1} = 130.669$$

$$\sigma_{B2} := \frac{M_{D2} \cdot 10^6}{S_{Blt}} \qquad \sigma_{B2} = 20.971$$

$$\sigma_{B3} := \frac{M_{D3} \cdot 10^6}{S_{Blt}} \qquad \sigma_{B3} = 10.724$$

$$\sigma_{B4} := \frac{1.3 \cdot M_{LLIM} \cdot 10^6}{S_{Bst}} \qquad \sigma_{B4} = 164.635$$

$$\sigma_{Btot} := \sigma_{B1} + \sigma_{B2} + \sigma_{B3} + \sigma_{B4} \qquad \sigma_{Btot} = 326.999$$

$$A_{beam} = 4.511 \times 10^4$$

8. Verify adequacy of section Mp (PNA in top flange)

$P_{rt} := 240$

$P_{rb} := 640$

$P_{sl} := .85 \cdot 30 \cdot b_s \cdot t_s \cdot 10^{-3}$ $\quad P_{sl} = 1.182 \times 10^4$

$P_{cf} := .345 \cdot t_t \cdot b_t$ $\quad P_{cf} = 2.422 \times 10^3$

$P_w := .345 \cdot t_w \cdot D$ $\quad P_w = 8.073 \times 10^3$

$P_{tf} := .345 \cdot t_b \cdot b_b$ $\quad P_{tf} = 5.068 \times 10^3$

Plastic force in girder:

$P_{cf} + P_w + P_{tf} = 1.556 \times 10^4$

Plastic force in girder tension flange and web

$P_{tf} + P_w = 1.314 \times 10^4$

Max. plastic force in slab

$P_{sl} + P_{rt} + P_{rb} = 1.27 \times 10^4$

Max. plastic force in slab + compr. flange:

$P_{sl} + P_{rt} + P_{rb} + P_{cf} = 1.512 \times 10^4$

Therefore, PNA is in the top flange. Since PNA is in the top flange:

$$y_{bar} := \frac{(t_t)}{2} \cdot \left(\frac{P_w + P_{tf} - P_{sl} - P_{rt} - P_{rb}}{P_{cf}} + 1 \right)$$ $\quad y_{bar} = 10.632 < 18$

$d_{rt} := t_s - d_p + t_h + y_{bar}$ $\quad d_{rt} = 172.632$

$d_{rb} := t_s - d + t_h + y_{bar}$ $\quad d_{rb} = 68.632$

$d_{sl} := \frac{t_s}{2} + t_h + y_{bar}$ $\quad d_{sl} = 130.632$

$d_{cf} := \frac{t_t}{2} - y_{bar}$ $\quad d_{cf} = -1.632$

$d_w := \frac{D}{2} + t_t - y_{bar}$ $\quad d_w = 907.368$

$d_{tf} := \frac{t_b}{2} + D + t_t - y_{bar}$ $\quad d_{tf} = 1.82 \times 10^3$

$$M_p := \left[\frac{P_{cf}}{2 \cdot t_t} \cdot \left[y_{bar}^{\,2} + \left(t_t - y_{bar}\right)^2\right] + P_{sl} \cdot d_{sl} + P_{rt} \cdot d_{rt} + P_{rb} \cdot d_{rb} + P_w \cdot d_w + P_{tf} \cdot d_{tf}\right] \cdot 10^{-3}$$

$M_p = 1.819 \times 10^4$

Check web slenderness

Web in compression = 0 at plastic moment.

9. Ductility check

(positive bending stress has already been found to be greater than fy)

$D_p := t_s + t_h + y_{bar}$ $\quad D_p = 225.632$

$D_{prime} := .7 \cdot \frac{\left(h + t_h + t_s\right)}{7.5}$ $\quad D_{prime} = 192.173$

$\frac{D_p}{D_{prime}} = 1.174$

Calculate composite section yield moment:

$$M_{ad} := S_{Bst} \cdot \left[345 - \frac{M_{D1} \cdot 10^6}{S_{Bnc}} - \frac{\left(M_{D2} + M_{D3}\right) \cdot 10^6}{S_{Blt}}\right] \cdot 10^{-6} \qquad M_{ad} = 7.551 \times 10^3$$

$M_y := M_{D1} + M_{D2} + M_{D3} + M_{ad}$ $\quad M_y = 1.27 \times 10^4$

$$M_n := \frac{5 \cdot M_p - .85 M_y}{4} + \frac{.55 M_y - M_p}{4} \cdot \left(\frac{D_p}{D_{prime}}\right) \qquad M_n = 1.675 \times 10^4$$

10. Check constructability

A. Web bend buckling

$k := 9 \cdot \left(\frac{D}{D_c}\right)^2$ $\quad k = 26.156$

$M_{Uconstr} := .95 \cdot 1.25 \cdot M_{D1}$ $\quad M_{Uconstr} = 4.688 \times 10^3$

$$f_c := \frac{M_{Uconstr} \cdot 10^3}{S_{Tnc}} \qquad f_c = 0.216$$

$$f_{cw} := f_c \cdot \left(\frac{D_c}{y_{Tnc}} \right) \qquad f_{cw} = 0.213$$

$$f_{cw} \text{ less than } \frac{.9 \cdot 200 \cdot 1.25 \cdot k}{\left(\frac{D}{t_w} \right)^2} = 0.307$$

B. Web shear resistance

$V_{D1} := 345 \qquad V_{D2} := 69.3 \qquad V_{D3} := 35.4 \qquad V_{LLIM} := 470$

Assume stiffener spacing equals web depth

$$k := 5 + \frac{5}{(1)^2} \qquad k = 10$$

Calculate buckling load coefficient for the web

$$\frac{D}{t_w} = 138.462 \text{ greater than } 1.38 \cdot \sqrt{\frac{200 \cdot k}{.345}} = 105.071$$

$$C := \frac{1.52 \cdot 200 \cdot k}{\left(\frac{D}{t_w} \right)^2 \cdot .345} \qquad C = 0.46$$

$$V_n := C \cdot .58 \cdot .345 \cdot D \cdot t_w \qquad V_n = 2.152 \times 10^3$$

$$V_{Uconstr} := .95 \cdot 1.25 \cdot V_{D1} \qquad V_{Uconstr} = 409.688$$

C. Check provisions of section 6.10.4.2.4 and 6.10.4.2.6 for construction stage

Lateral torsional buckling limit with tension flange free to rotate (6.10.4.2.6)

$\frac{2\cdot(D_c)}{t_w} = 162.44$ greater than $4.64\sqrt{\frac{200}{f_c}} = 141.072$ so $R_b < 1$

$a_r := \frac{2\cdot D_c\cdot t_w}{t_t\cdot b_t}$ $a_r = 3.911$

The load shedding factor varies depending upon the stress.

$f_c(x) := \frac{1.25\cdot 1000\cdot M_{D1}}{S_{Tnc}}\cdot 4\cdot\left(1 - \frac{x}{45.72}\right)\cdot\frac{x}{45.72}$ E := 200

$R_{b1}(x) := 1 - \left(\frac{a_r}{1200 + 300\cdot a_r}\right)\cdot\left(\frac{2\cdot D_c}{t_w} - 4.64\cdot\sqrt{\frac{E}{f_c(x)}}\right)$ $R_h := 1$

The formula can predict values greater than 1 for small fc, and is singular for fc=0, so a logic statement is needed here.

$R_b(x) := \text{if}\left(f_c(x) > 0, \text{if}\left(R_{b1}(x) < 1, R_{b1}(x), 1\right), 1\right)$

First, check maximum tension stress, which is likely to be o.k.

$f_T := \frac{M_{Uconstr}\cdot 10^3}{S_{Bnc}}$ $f_T = 0.155$

$F_{nTen} := R_b(22.86)\cdot .345$

greater than $F_{nTen} = 0.331$

To address lateral torsional buckling issues, we need certain basic section properties:

$r_T := \frac{b_t}{\sqrt{12}}$ $F_y := 0.345$

$J := \frac{b_t\cdot t_t^3 + t_w^3\cdot D + b_b\cdot t_b^3}{3}$ $J = 5.387\times 10^6$

$I_{yc} := \frac{t_t\cdot b_t^3}{12}$ $I_{yc} = 8.898\times 10^7$

$$L_r := 4.44\sqrt{\frac{I_{yc}\cdot(D + t_t + t_b)\cdot E}{S_{Tnc}\cdot F_y}} \qquad L_r = 9.302\times 10^3$$

$$L_p := 1.76\cdot r_T\cdot\sqrt{\frac{E}{F_y}} \qquad L_p = 4770.8$$

$$M_{ync} := S_{Tnc}\cdot F_y \qquad M_{ync} = 7.476\times 10^6$$

Calculate the nominal moment resistance, using the lateral torsional buckling equations for the tension flange free to rotate. (Section 6.10.4.2.6)

$$M_{n1}(x) := R_b(x)\cdot R_h\cdot M_{ync} \qquad \text{(Strength controlled by yielding)}$$

$$M_{n2}(C_b, x, L_b) := C_b\cdot R_b(x)\cdot R_h\cdot M_{ync}\cdot\left[1 - 0.5\cdot\left(\frac{L_b - L_p}{L_r - L_p}\right)\right] \qquad \text{(Inelastic buckling)}$$

$$M_{n3}(C_b, x, L_b) := C_b\cdot R_b(x)\cdot R_h\cdot\frac{M_{ync}}{2}\cdot\left(\frac{L_r}{L_b}\right)^2 \qquad \text{(Elastic buckling)}$$

$$M_n(C_b, x, L_b) := \text{if}\left(L_b < L_r, \text{if}\left(M_{n2}(C_b, x, L_b) < M_{n1}(x), M_{n2}(C_b, x, L_b), M_{n1}(x)\right), M_{n3}(C_b, x, L_b)\right)$$

$$F_n(C_b, x, L_b) := \frac{M_n(C_b, x, L_b)}{S_{Tnc}}$$

Base maximum bracing length at center of beam upon the stress at midspan, and upon the assumption that the moment gradient is small near midspan, so Cb is about 1. Use rough calculations to estimate Cb for adjacent sections.

$$L_b := 0, 100 .. 12000$$

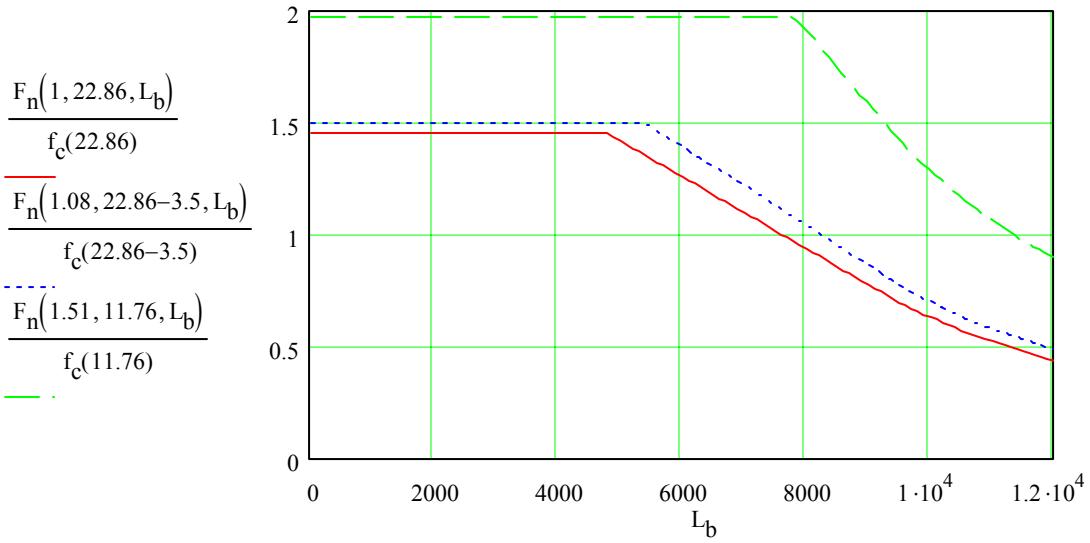

In the plots, the maximum unbraced lengths are reached when the ratios cross 1. As we move from midspan toward the end of the beam, the moment gradient, and hence Cb increases.

From the plots, midspan bracing should be at 7.5 m straddling the centerline. A side brace spaced 8 m further out completes the bracing. The resulting bracing spacing is 11.11 m, 8 m, 7.5 m, 8 m, 11.11 m from end of span to end of span.

Flange buckling limit stress (6.10.4.2.4):

$$F_{cr} := \frac{1.904200}{\left(\frac{b_t}{2 \cdot t_t}\right)^2 \cdot \sqrt{\frac{2 \cdot (D_c)}{t_w}}}$$

$F_{cr} = 0.255$ less than $F_y := .345$ can control the size of the compression flange.

The actual flange compressive stress is roughly $f_c(22.86) = 0.228$ O. K.

11. Web Fatigue

a) Check the web buckling provision

$$f_{cf} := \left(\frac{M_{D1}}{S_{Tnc}} + \frac{M_{D2} + M_{D3}}{S_{Tlt}} + \frac{2 \cdot M_{FatLLIM}}{S_{Tst}}\right) \cdot 10^3 \qquad f_{cf} = 0.225$$

$$f_{tf} := \left(\frac{M_{D1}}{S_{Bnc}} + \frac{M_{D2} + M_{D3}}{S_{Blt}} + \frac{2 \cdot M_{FatLLIM}}{S_{Bst}}\right) \cdot 10^3 \qquad f_{tf} = 0.242$$

So for web fatigue:

$$D_c := \left(D + t_t + t_b\right)\cdot\frac{f_{cf}}{f_{cf} + f_{tf}} - t_t \qquad D_c = 869.286$$

$$k := 9\cdot\left(\frac{D + t_t + t_b}{D_c}\right)^2 \qquad k = 40.499$$

For the section at present:

$$\frac{D}{t_w} = 138.462 \quad \text{is not greater than} \quad .95\cdot\sqrt{\frac{k\cdot 200}{.345}} = 145.562$$

So fcf must be less than .345

If it were greater, the permissible flange stress must be less than the following

$$f_{cf} \text{ must be less than } .9\cdot k\cdot 200\left(\frac{t_w}{D}\right)^2 = 0.38$$

b) Check the limiting stress in shear for web fatigue

$$v_{cf} := .58\cdot C\cdot .345 \qquad v_{cf} = 0.092$$

$$V_{FT} := 286$$

$$V_{FatLLIM} := .75\cdot 1.15\cdot .826\cdot\frac{V_{FT}}{1.2} \qquad V_{FatLLIM} = 169.795$$

$$V := V_{D1} + V_{D2} + V_{D3} + 2\cdot V_{FatLLIM} \qquad V = 789.289$$

$$v := \frac{V}{D\cdot t_w} \qquad v = 0.034$$

12. Check strength limit state for shear

$$V_u := 1.25\cdot\left(V_{D1} + V_{D3}\right) + 1.5\cdot V_{D2} + 1.75\cdot V_{LLIM} \qquad V_u = 1.402\times 10^3$$

$$V_p := .58\cdot .345\cdot D\cdot t_w \qquad V_p = 4.682\times 10^3$$

$$V_r := V_p \cdot \left[C + \frac{.87 \cdot (1 - C)}{\sqrt{1 + 1^2}} \right] \qquad V_r = 3.709 \times 10^3$$

There is more than adequate shear resistance here. In the end panel, post-buckling resistance cannot be used, so

$$V_n := C \cdot V_p \qquad V_n = 2.152 \times 10^3$$

Skip design of shear connectors for this analysis.

13. Transverse stiffener design

b_t greater than $b_t := 50 + \frac{D}{30}$ $\qquad b_t = 110$

lower limit

t_p greater than $\frac{b_t}{16} = 6.875$ greater than $\frac{b_b}{64} = 8.828$ so $t_p := 9$

$$J := 2.5 \cdot (1)^2 - 2$$

$I_t := D \cdot t_w^3 \cdot J$ $\qquad I_t = 1.977 \times 10^6$

lower limit for I

$B := 2.4$ Say $t_p := 9$ $\quad b_t := 125$

$F_{cr} := \frac{.311 \cdot 200}{\left(\frac{b_t}{t_p}\right)^2}$ less than .345 $\qquad F_{cr} = 0.322$

A_s greater than $\left[.15 \cdot B \cdot \frac{D}{t_w} \cdot (1 - C) \cdot \left(\frac{V_u}{V_r} \right) - 18 \right] \cdot \frac{.345}{F_{cr}} \cdot t_w^2 = -1.414 \times 10^3$

There is no minimum area requirement.

$I := \frac{t_p \cdot b_t^3}{3}$ $\qquad I = 5.859 \times 10^6$

14. Bearing stiffener design

$\frac{b_t}{t_p}$ must be less than $.48\cdot\sqrt{\frac{200}{.345}} = 11.557$

$A_{pn} = 2(11\cdot t_p - 40)\cdot t_p$ greater than $\frac{V_u}{1\cdot.345} = 4.064\times 10^3$ $t_p := 15.5$

performed on calculator

Say $t_p := 17$ $b_t := 170$ $\frac{b_t}{t_p} = 10$

$A := 2\cdot b_t\cdot t_p + 18\cdot t_w^2$ $A = 8.822\times 10^3$

$I := \frac{t_p\cdot(2\cdot b_t + t_w)^3}{12}$ $I = 6.231\times 10^7$

$r := \sqrt{\frac{I}{A}}$ $r = 84.045$

$\lambda := \left(\frac{.75\cdot D}{r\cdot\pi}\right)^2\cdot\frac{.345}{200}$ $\lambda = 0.045$ $\lambda < 2.25$

$\phi P_n := .66^{\lambda}\cdot.345\cdot A$ $\phi P_n = 2.987\times 10^3$

ϕP_n greater than $V_u = 1.402\times 10^3$

15. Check fatigue and fracture provisions for details

a) Stress range at longitudinal welds. Category B

$\Delta f_{tf} := \frac{M_{FatLLIM}\cdot 10^3}{S_{Bst}}$ $\Delta f_{tf} = 0.04$

$N := 186\cdot 10^6$ cycles

For category B, $\Delta F_{TH} := .11$ so stress is below threshold

APPENDIX D
CONCRETE DECK PROPORTIONS

For facilitate comparisons of the steel girder designs using the AASHTO ASD and LRFD bridge codes, design of the concrete decks were varied only with the number of girders per bridge. Therefore, ASD and LRFD designs for both span lengths included the same concrete deck proportions.

6 Girder Deck Design:

Interior Slab Thickness, t_s = 205 mm
Overhang Slab Thickness, t_o = 230 mm

Transverse Bottom Reinforcement:	No. 15 bar @ 225 mm	A_s = 0.89 mm^2/mm
Transverse Top Reinforcement:	No. 15 bar @ 225 mm	A_s = 0.89 mm^2/mm
Longitudinal Bottom Reinforcement:	No. 10 bar @ 150 mm	A_s = 0.67 mm^2/mm
Longitudinal Top Reinforcement:	No. 10 bar @ 450 mm	A_s = 0.22 mm^2/mm

5 Girder Deck Design:

Interior Slab Thickness, t_s = 225 mm
Overhang Slab Thickness, t_o = 250 mm

Transverse Bottom Reinforcement:	No. 20 bar @ 300 mm	A_s = 1.00 mm^2/mm
Transverse Top Reinforcement:	No. 15 bar @ 225 mm	A_s = 0.89 mm^2/mm
Longitudinal Bottom Reinforcement:	No. 10 bar @ 150 mm	A_s = 0.67 mm^2/mm
Longitudinal Top Reinforcement:	No. 10 bar @ 450 mm	A_s = 0.22 mm^2/mm

4 Girder Deck Design:

Interior Slab Thickness, t_s = 255 mm
Overhang Slab Thickness, t_o = 280 mm

Transverse Bottom Reinforcement:	No. 20 bar @ 300 mm	A_s = 1.00 mm^2/mm
Transverse Top Reinforcement:	No. 15 bar @ 225 mm	A_s = 0.89 mm^2/mm
Longitudinal Bottom Reinforcement:	No. 10 bar @ 150 mm	A_s = 0.67 mm^2/mm
Longitudinal Top Reinforcement:	No. 10 bar @ 400 mm	A_s = 0.25 mm^2/mm